



Preparation, characterization, *in vitro* drug release, and cellular interactions of tailored paclitaxel releasing polyethylene oxide films for drug-coated balloons



Jordan A. Anderson^a, Sujan Lamichhane^a, Tyler Remund^b, Patrick Kelly^c, Gopinath Mani^{a,*}

^a Biomedical Engineering, The University of South Dakota, 4800 North Career Avenue, Sioux Falls, SD 57107, USA

^b Sanford Research, 2301 East 60th Street North, Sioux Falls, SD 57104, USA

^c Sanford Health, 1305 West 18th Street, Sioux Falls, SD 57105, USA

ARTICLE INFO

Article history:

Received 1 April 2015

Received in revised form 3 September 2015

Accepted 28 September 2015

Available online 30 September 2015

Keywords:

Drug-coated balloon
Cardiovascular disease
Restenosis
Polyethylene oxide
Smooth muscle cells

ABSTRACT

Drug-coated balloons (DCBs) are used to treat various cardiovascular diseases. Currently available DCBs carry drug on the balloon surface either solely or using different carriers. Several studies have shown that a significant amount of drug is lost in the blood stream during balloon tracking to deliver only a sub-therapeutic level of drug at the treatment site. This research is focused on developing paclitaxel (PAT) loaded polyethylene oxide (PEO) films (PAT-PEO) as a controlled drug delivery carrier for DCBs. An array of PAT-PEO films were developed in this study to provide tailored release of >90% of drug only at specific time intervals, which is the time frame required for carrying out balloon-based therapy. The characterizations of PAT-PEO films using SEM, FTIR, and DSC showed that the films developed were homogenous and the PAT was molecularly dispersed in the PEO matrix. Mechanical tests showed that most PAT-PEO films developed were flexible and ductile, with yield and tensile strengths not affected after PAT incorporation. The viability, proliferation, morphology, and phenotype of smooth muscle cells (SMCs) interacted with control-PEO and PAT-PEO films were investigated. All control-PEO and PAT-PEO films showed a significant inhibitory effect on the growth of SMCs, with the degree of inhibition strongly dependent on the w/v% of the polymer used. The PAT-PEO coating was produced on the balloons. The integrity of PAT-PEO coating was well maintained without any mechanical defects occurring during balloon inflation or deflation. The drug release studies showed that only 15% of the total PAT loaded was released from the balloons within the initial 1 min (typical balloon tracking time), whereas 80% of the PAT was released between 1 min and 4 min (typical balloon treatment time). Thus, this study demonstrated the use of PEO as an alternate drug delivery system for the balloons.

Statement of Significance

Atherosclerosis is primarily responsible for cardiovascular diseases (CVDs) in millions of patients every year. Drug-coated balloons (DCBs) are commonly used to treat various CVDs. However, in several currently used DCBs, a significant amount of drug is lost in the blood stream during balloon tracking to deliver only a sub-therapeutic level of drug at the treatment site. In this study, paclitaxel containing polyethylene oxide (PEO) films were developed to provide unique advantages including drug release profiles specifically tailored for balloon-based therapy, homogeneous films with molecularly dispersed drug, flexible and ductile films, and exhibits significant inhibitory effect on smooth muscle cell growth. Thus, this study demonstrated the use of PEO as an alternate drug delivery platform for DCBs to improve its efficacy.

© 2015 Acta Materialia Inc. Published by Elsevier Ltd. This is an open access article under the CC BY-NC-ND license (<http://creativecommons.org/licenses/by-nc-nd/4.0/>).

1. Introduction

Drug-coated balloons (DCBs) are currently used to treat various cardiovascular diseases by opening up the blocked arteries and delivering antiproliferative therapeutic drugs locally to prevent

* Corresponding author.

E-mail address: Gopinath.Mani@usd.edu (G. Mani).

restenosis (artery renarrowing) [11–11]. Most DCBs currently available are coated with drugs either directly without using any carriers (a carrier is a substance that provides a platform to carry drug on the balloon surface and to deliver it in a controlled manner) or using different types of carriers [11,12]. The carriers that are currently used in DCBs include urea, polysorbate emulsifier, shellac resin, iopromide contrast medium, and butyryl trihexyl citrate plasticizer [11,12]. Most of these carriers are chosen on the basis of their usefulness to improve drug penetration into the tissue and not on whether they assist in delivering significant amount of drug at the treatment site of diseased portion of the artery. The major limitation of currently available DCBs is the delivery of drug from the balloons is not controlled effectively in order to avoid drug loss during balloon tracking and to rapidly deliver a therapeutic level of drug at the treatment site [11–14]. It has been reported that a significant amount of drug (up to 80%) is lost in the blood stream even before the balloon is tracked to the treatment site [11–14]. Also, during the short balloon inflation time (2–3 min), the drug is not rapidly transferred from the balloon to the tissue [11–14]. Hence, in many cases, only a subtherapeutic level of drug is delivered at the treatment site [11–14]. Therefore, a great need has arisen to control the delivery of drug from the balloons in such a way that the drug loss during its transit to the treatment site should be as minimal as possible, and then, all or most of the drug from the balloon should be immediately released at the treatment site during the short time of balloon inflation. With this as the goal, in this study, we have developed paclitaxel (PAT) loaded polyethylene oxide (PEO) films to provide drug release profiles that are well-suited for use in DCBs. The w/v% of PEO and wt% of PAT were varied to obtain different groups of PAT–PEO films that show tailored release of >90% of drug only at specific time intervals. The various PAT–PEO films developed in this study were characterized for their drug loading and release profiles, surface and bulk properties, mechanical properties, and smooth muscle cell (SMC) growth inhibitory effects. Also, the PAT–PEO coating produced on the balloons was investigated for its coating integrity and drug release properties. The results of PAT–PEO coated balloons were then compared to that of control DCBs, which were prepared using PAT only (without any carriers) and currently used drug-carrier combinations such as PAT–urea, PAT–polysorbate/sorbitol, PAT–shellac, and PAT–contrast agent.

2. Materials and methods

2.1. Materials

Poly(ethylene oxide) (PEO, average M_v 100,000), ethanol (200 proof), methanol, phosphate-buffered saline with 0.05 wt% tween-20 (PBS/T-20), Dulbecco's phosphate-buffered saline (DPBS), fluorescein diacetate (FDA), tris-buffered saline (TBS), propidium iodide (PI), HPLC-grade water and acetonitrile, urea, polysorbate, sorbitol, and shellac were all purchased from Sigma–Aldrich (USA). Iodixanol (contrast agent) was purchased from GE Healthcare Inc. (Princeton,

NJ). Paclitaxel (PAT) was purchased from ChemieTek (Indianapolis, IA). All chemicals purchased were used as received.

2.2. Preparation of PAT loaded PEO films and control PEO films

PAT loaded PEO (PAT–PEO) films were prepared in this study using the solvent casting method. Initially, the PEO (10%, w/v) was dissolved in de-ionized water (di-H₂O) by stirring the polymer in the solvent at 200 rpm for 6 h. In parallel, a solution of PAT was prepared in ethanol by sonicating the drug in the solvent for 5 min thrice. The PAT solution (10 mg/mL) prepared was then added dropwise into the PEO solution at 1.5 wt%, and the drug-polymer mixture was stirred at 200 rpm for 18 h. The drug-polymer mixture solution was then poured into a petridish (8.8 cm in diameter) and heated in an oven at 50 °C under vacuum (–20 inHg) for 48 h. The oven was then turned off and the samples were left inside the oven for 30 min to slowly cool the samples. The petridish was then removed from the oven and the PAT–PEO films formed were peeled off using a razor. The PAT–PEO films were then cut into specimens of varying sizes for performing different characterizations.

Similar experiments were carried out for preparing PAT–PEO films with 15, 20, and 25 w/v% of PEO. However, there was no change made in the concentration (10 mg/mL) or volume (3 mL) of PAT solution that was added to the different w/v% PEO. This led to PAT loadings of 1.0, 0.75, and 0.6 wt% in PEO (15%, w/v), PEO (20%, w/v), and PEO (25%, w/v) films, respectively. Thus, the PAT–PEO films prepared in this study with 10 w/v% of PEO and 1.5 wt% of PAT, 15 w/v% of PEO and 1.0 wt% of PAT, 20 w/v% of PEO and 0.75 wt% of PAT, and 25 w/v% of PEO and 0.6 wt% of PAT are referred to as PAT–PEO-10, PAT–PEO-15, PAT–PEO-20, and PAT–PEO-25, respectively. Table 1A shows the polymer weight, solvent volume, drug solution volume, and stirring speed used in the preparation of these four different groups of PAT–PEO films.

Control PEO films (without PAT loaded) were also prepared at four different w/v% (10, 15, 20, and 25). The protocols for preparing these control films were similar to the above mentioned procedure without the addition of PAT (Table 1B).

2.3. Drug-elution studies

For the drug-elution studies, the PAT–PEO film specimens (0.5 cm × 0.5 cm) were immersed in 25 mL of PBS/T-20 solution and incubated in a circulating water bath (Thermo Scientific, USA) at 37 °C. As a standard protocol, Tween-20, a non-ionic surfactant, was added in the release medium to increase the solubility of PAT in PBS and to maintain sink conditions [15,16]. At each pre-determined time point (30 s, 1 min, 2 min, 3 min, 5 min, and 7 min), the films were taken out of the solution and transferred to a fresh PBS/T-20 solution. Due to the inherent water solubility of PEO, the films started to turn loose at different time points depending on the group of PAT–PEO film. When the films turned too loose to handle at a time point, it was permanently placed in the PBS/T-20 solution used for that respective time point without

Table 1A

Polymer weight, solvent volume, drug solution volume, and stirring speed used in the preparation of four different groups of PAT–PEO films.

PAT–PEO film groups	PEO (wt/vol%)	PAT (wt%)	Weight of PEO (grams)	Volume of di-H ₂ O (mL)	Volume of PAT solution in mL (drug concentration is 10 mg/mL)	Stirring speed* during mixing (rpm)
PAT–PEO-10	10	1.5	2	17	3	200
PAT–PEO-15	15	1	3	17	3	200
PAT–PEO-20	20	0.75	4	17	3	175
PAT–PEO-25	25	0.6	5	17	3	50

* Stirring speed was decided depending on the viscosity of the solution. For instance, a stirring speed of 200 rpm was required for an even mixing of PAT–PEO-10 solution. However, for PAT–PEO-25, which is highly viscous when compared to other PAT–PEO solutions, the stirring speed has to be significantly reduced to 50 rpm for even mixing.

Table 1B

Polymer weight, solvent volume, and stirring speed used in the preparation of four different groups of control PEO films.

Control PEO film groups	PEO (wt/vol%)	PAT (wt%)	Weight of PEO (grams)	Volume of di-H ₂ O (mL)	Volume of PAT solution in mL (drug concentration is 10 mg/mL)	Stirring speed during mixing (rpm)
PEO-10	10	0	2	20	0	200
PEO-15	15	0	3	20	0	200
PEO-20	20	0	4	20	0	175
PEO-25	25	0	5	20	0	50

transferring to the next time point. The time point at which the film was permanently placed in the PBS/T-20 solution was regarded as the final time point for that particular group of PAT-PEO film. The final time points for PAT-PEO-10, PAT-PEO-15, PAT-PEO-20, and PAT-PEO-25 groups were 2 min, 5 min, 5 min, and 7 min, respectively. The PBS/T-20 samples collected at each time point were then used for determining the amount of PAT released using high performance liquid chromatography (HPLC). Prior to HPLC analysis, 1 mL of ethanol was added to the plastic tubes in which the PBS/T-20 samples were collected and shaken well for 30 s. This ethanol addition step was carried out as a standard procedure to remove any PAT that was physically bound to the plastic tube surfaces [15,16]. The HPLC method for determining PAT released was carried out as we reported previously [17,18].

2.4. Characterization of PAT-PEO and control PEO films

All PAT-PEO and control PEO films prepared in this study were characterized using scanning electron microscopy (SEM), optical surface profilometry (OSP), Fourier transform infrared spectroscopy (FTIR), and differential scanning calorimetry (DSC). A Quanta 450 SEM (FEI, USA) was used to image the morphology of surfaces as well as the cross-sections of PAT-PEO and control PEO films. For SEM imaging, 10 kV and 30 kV accelerating voltages were used for obtaining surface and cross-sectional images, respectively. Prior to SEM analysis, the films were sputter-coated with a 15 nm thick gold-palladium to avoid surface charging. A Wyko NT8000 OSP (Bruker Corporation; operated at Michigan Metrology, LLC) was used in this study to obtain 3D topography images of control PEO and PAT-PEO specimens. A Nicolet 6700 FTIR spectroscopy (Thermo Scientific, USA) equipped with an attenuated total reflection (ATR) accessory was used to characterize the surfaces of PAT-PEO and control PEO films. The FTIR spectra of PAT and PEO in powder forms were also obtained. All FTIR spectra were collected at 1024 scans with a spectral resolution of 4 cm⁻¹. All collected spectra were analyzed using OMNIC software. A Q200 DSC (TA instruments, New Castle, DE) was used in this study to characterize all PAT-PEO and control PEO films. PEO and PAT in powder forms were also characterized using DSC. For this characterization, a sample weighing 8–10 mg was sealed in an aluminum pan and heated to 300 °C at a scan rate of 10 °C/min. As a reference, an empty aluminum pan was used. All DSC measurements were carried out under nitrogen gas at a flow rate of 40 mL/min.

2.5. Mechanical testing of PAT-PEO and control PEO films

An MTS insight electromechanical instrument (MTS System Corp., Eden Prairie, MN) was used in this study to characterize all PAT-PEO and control PEO film specimens (1 cm × 7 cm, *n* = 3 for each sample group). The thickness of the specimens was determined using SEM. The specimens were gripped at a length of 1 cm from each end and stretched to failure using a 100N load cell at 50 mm/min extension rate. A TestWorks 4 software was used to determine the elastic modulus, strain at break, peak load, and tensile strength from the stress-strain curves obtained for the films.

2.6. Characterization of PAT-PEO films post drug-elution studies

To determine the drug delivery mechanism, the PAT-PEO films used in the drug-elution studies were characterized using FTIR and DSC to observe the changes occurred in the chemical composition and crystallinity of the films, respectively. Also, the films were immersed in 2 mL of PBS/T-20 at 37 °C, and real-time images were obtained using phase contrast microscopy to observe the morphological changes of the films.

2.7. Smooth muscle cell (SMC) cultures

Human aortic smooth muscle cells (HASMCs, catalog No. 354-05a) and smooth muscle cell growth medium (catalog No. 311-500) were obtained from Cell Applications (San Diego, CA). The cells were cultured in the growth medium at 37 °C in a humidified 5% CO₂ incubator. The cells obtained from passages four to six were used in this study. Initially, a density of 15 × 10³ cells (in 1000 µL of growth medium) was allowed to grow in the wells of a 24-well tissue culture plate for 24 h. The used media were then removed and 1000 µL of fresh growth media were added to the wells. Then, PAT-PEO or control-PEO film specimens (1 cm × 1 cm) were added to the cells grown in the wells. After 18 h (on day-1), the used media were removed and 1000 µL of fresh growth media were added to the wells. The media were changed again on day-3 and day-5. A control experiment was also carried out as the cells were allowed to grow in the wells in the absence of either PAT-PEO or control-PEO films.

2.7.1. Smooth muscle cell viability and proliferation

The resazurin cell viability assay kit (trademark name AlamarBlue) was purchased from Biotium (Hayward, CA) and used to quantitatively measure the viability and proliferation of cells [19,20]. At pre-determined time points (day-1, 3, and 5), the used media were removed and a solution containing the mixture of resazurin (100 µL) and cell culture medium (900 µL) was added to the cells. Then, the cells were incubated in the solution at 37 °C in the dark for 6 h. The fluorescence of the solution was measured using a Tecan Infinite® M200 microplate reader (Tecan Group Ltd., Mannedorf, Switzerland) at excitation and emission wavelengths of 530 nm and 590 nm, respectively. The fluorescence of the blanks (cell growth medium and resazurin, without cells) was also obtained and the value was subtracted from the fluorescence values of the experimental samples. The values reported here are the corrected fluorescence values. For the cell viability and proliferation study, three samples were used for each of the eight groups (four groups of PAT-PEO and four groups of control PEO) at each time point (1, 3, and 5 days). Therefore, 72 samples were used in this part of the study.

2.7.2. Smooth muscle cell morphology

The morphology of SMCs was characterized as we reported previously [19,20]. Briefly, a stock solution of fluorescein diacetate (FDA) was prepared at a concentration of 1 mg/mL in acetone. The working solution was prepared by adding 100 µL of the prepared FDA stock solution to 900 µL of DPBS. After 1, 3, and 5 days,

the used media were removed, and a solution containing 60 μL of the FDA working solution and 1000 μL of DPBS was added to the cells. Then, the cells were incubated in the solution at -20°C in the dark for 15 min. An Axiovert 200 M inverted fluorescence microscope (Carl Zeiss Microscopy, Thornwood, NY) was used to image the cells. For the morphology study also, three samples were used for each of the eight sample groups at each of the three time points. Hence, 72 samples were used for this part of the study as well. The fluorescence images were obtained at a minimum of four different spots on each sample and the representative images of each sample group are provided here. The SMC size was quantitatively determined by calculating its aspect ratio using the ImageJ software. The aspect ratio of cells was defined as the ratio of length of major axis to the length of minor axis, with 1.0 being a complete circle. For each experimental group at each time point, three images were used for analysis. In each image, an aspect ratio of at least 10 cells was calculated. Hence, a total of 30 cells per group per time point was measured for the analysis.

2.7.3. Smooth muscle cell phenotype

Triton X-100, goat serum, α -actin antibody (1A4), and goat anti-mouse IgG-FITC were all purchased from Santa Cruz Biotechnology (Santa Cruz, CA). The SMC phenotype was characterized as we reported previously [20]. Briefly, the cells treated with control PEO films or PAT-PEO films or no films (control wells) were allowed to grow for 3 days. Then, the cells were washed with DPBS twice and fixed using 4% paraformaldehyde (Affymetrix, Santa Clara, CA) at room temperature (RT) for 10 min. The cells were then washed with DPBS five times for 3 min each and incubated in a permeabilizing solution (0.1% Triton X-100 in tris-buffered saline) for 25 min at RT. The cells were subsequently washed with DPBS followed by incubating in blocking buffer (10% of goat serum in permeabilizing solution) for 25 min at RT. Then, the cells were washed with DPBS and incubated in α -actin primary antibody diluted 1:50 with 1.5% goat serum in DPBS for 90 min at RT. After washing with DPBS five times for 5 min each, the cells were incubated in goat anti-mouse IgG-FITC secondary antibody diluted 1:75 with 1.5% goat serum in DPBS for 60 min at RT in the dark. The cells were then washed with DPBS five times for 5 min each and incubated in 2% propidium iodide (PI) in DPBS for 15 min at RT in the dark to stain the nucleus. A laser scanning confocal microscope (Nikon, Melville, NY) was then used to image the cells. The immunofluorescence microscopy images obtained were analyzed for the quantification of smooth muscle α -actin in the cells using ImageJ software as described previously [21–23]. Briefly, the fluorescence intensity of the green color stained α -actin was measured. Also, the fluorescence intensity of the background (spots in the images where there are no cells) was measured. Once the integrated density of the cell was calculated, the corrected total cell fluorescence (CTCF) was determined using the following formula: $\text{CTCF} = \text{Integrated density} - (\text{Area of selected cell} \times \text{Mean fluorescence of background readings})$. The CTCF determined was used as a proxy for the amount of SM alpha-actin in the cells as described previously [21–23]. For each group, at least 15 cells were used for analysis.

2.8. Preparation of PAT-PEO coating on balloons

The PAT-PEO solution was prepared as described in the Section 2.2 with 10 w/v% of PEO and 4.5 wt% of PAT. Angioplasty balloon catheters (ev3 Inc., USA) of 2 mm in diameter \times 20 mm in length were used for the experiments. The balloons were initially inflated with an air pressure of 6–8 atm. Then, the inflated balloons were dipped in the prepared PAT-PEO solution (PAT concentration – 4.5 mg/mL) for 1 min followed by transferring them into an oven and heat treated in air at 50°C for 1 h. The

balloons were then taken out and dipped again in PAT-PEO solution for 15 s followed by heat treatment in air at 50°C for 1 h. This step was again repeated twice.

2.9. Preparation of control DCBs using currently available DCB coating combinations

The currently available coating combinations of DCBs include PAT only (without any carriers), and drug-carrier combinations such as PAT-urea, PAT-polysorbate/sorbitol, PAT-shellac, and PAT-contrast agent [24]. In this study, five control DCBs were prepared using these coating combinations. Except the control PAT only (without any carrier), all other drug-carrier combination solutions were prepared with a ratio of 1:1 (drug:carrier). The solvents used for preparing these solutions are either ethanol only (for PAT only and PAT-shellac) or ethanol:di- H_2O (50:50, v/v, for PAT-urea, PAT-polysorbate/sorbitol, and PAT-contrast agent). The concentration of PAT in all these solutions was kept as 4.5 mg/mL (the same PAT concentration used in PEO formulation as listed in Section 2.8). The balloons were coated with these solutions using the same dip coating procedure as described in Section 2.8.

2.10. SEM imaging of PAT-PEO coated balloons and control DCBs

The PAT-PEO coated balloons (Section 2.8) and the five control DCBs (Section 2.9) prepared were imaged using a SEM at three different positions including as-coated position, deflated position, and inflated position. Also, a bare balloon without any coatings was imaged in its inflated and deflated positions. An accelerated voltage of 1 kV was used to obtain the images at several different locations of the balloons.

2.11. Drug-elution studies of PAT-PEO coated balloons and control DCBs

The PAT-PEO coated balloons and control DCBs were deflated prior to drug-elution studies. Then, the deflated balloons were immersed in 50 mL of PBS/T-20 solution and incubated in a circulating water bath at 37°C . The balloons were removed from the solution and transferred to a fresh PBS/T-20 solution at pre-determined time points (30 s, 1 min, 2 min, 3 min, 4 min, 5 min, and 7 min). After the 1 min time point, the balloons were inflated with an air pressure of 6–8 atm and remained inflated for the time points thereafter. After 7 min, the balloons were taken out and sonicated in a 20 mL solution containing di- H_2O and ethanol (50:50, v/v) for 1 min to remove any residual drug present on the balloon. All solutions collected were analyzed for the amount of PAT released using HPLC.

2.12. Statistical analysis

All experiments conducted in this study were repeated at least thrice using different film batches. The experimental data collected in this study are presented as mean \pm standard deviation. A one-way analysis of variance (ANOVA) was used to determine the statistical significance at $p < 0.05$.

3. Results

3.1. Drug release from PAT-PEO films

Fig. 1A shows the percentage of PAT released at different time point intervals for the four different groups of PAT-PEO films prepared in this study. For PAT-PEO-10, the percentage of drug released was less than 3% for up to 1 min. However, the remaining

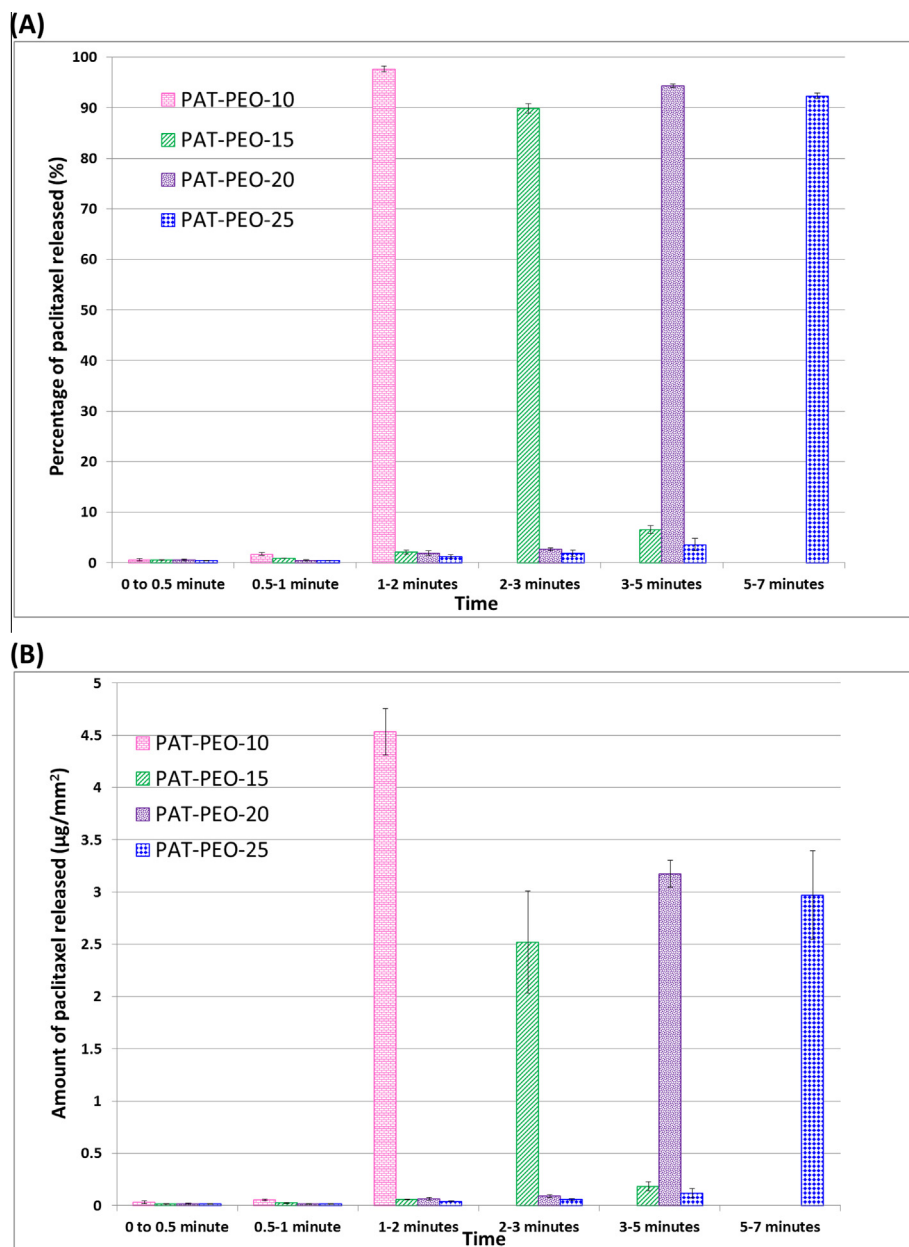


Fig. 1. Percentage (A) and amount (B) of paclitaxel released from PAT-PEO-10, PAT-PEO-15, PAT-PEO-20, and PAT-PEO-25 films.

~97% of the drug was released from this group of films between 1 min and 2 min. For PAT-PEO-15, only <4% of the drug was released by 2 min. However, the remaining ~90% of the drug was released from this group of films between 2 min and 3 min. For PAT-PEO-20, only ~6% of the drug was released for up to 3 min. However, the remaining ~94% of the drug was released from this group of films between 3 min and 5 min. Similarly, for

PAT-PEO-25, only <8% of the drug was released for up to 5 min. However, the remaining ~92% of the drug was released from this group of films between 5 min and 7 min. These results strongly demonstrated that the release of PAT from PEO films can be tailored to deliver ≥90% of drug only at specific time intervals of interest with <10% of the drug released at any other time points.

The total amount of PAT loaded in different groups of PAT-PEO films is provided in Table 1C. Fig. 1B shows the amount of drug released from four different groups of PAT-PEO films at different time points. For PAT-PEO-10, a drug dose of 4.5 ± 0.2 µg/mm² was released between 1 min and 2 min. Similarly, for PAT-PEO-15, PAT-PEO-20, and PAT-PEO-25, the drug doses of 2.5 ± 0.5 µg/mm², 3.2 ± 0.1 µg/mm², and 3.0 ± 0.4 µg/mm² were released between 2–3 min, 3–5 min, and 5–7 min, respectively. Only a trace amount of drug (<0.3 µg/mm²) was released from all these groups of films at any other time points used in the study. Several clinical studies in the literature have previously shown that a dose of

Table 1C

Total amount of drug (µg/mm²) loaded in PAT-PEO films.

Sample group	Drug loaded (µg/mm ²)
PAT-PEO-10	4.6 ± 0.2
PAT-PEO-15	2.8 ± 0.5
PAT-PEO-20	3.4 ± 0.2
PAT-PEO-25	3.2 ± 0.5

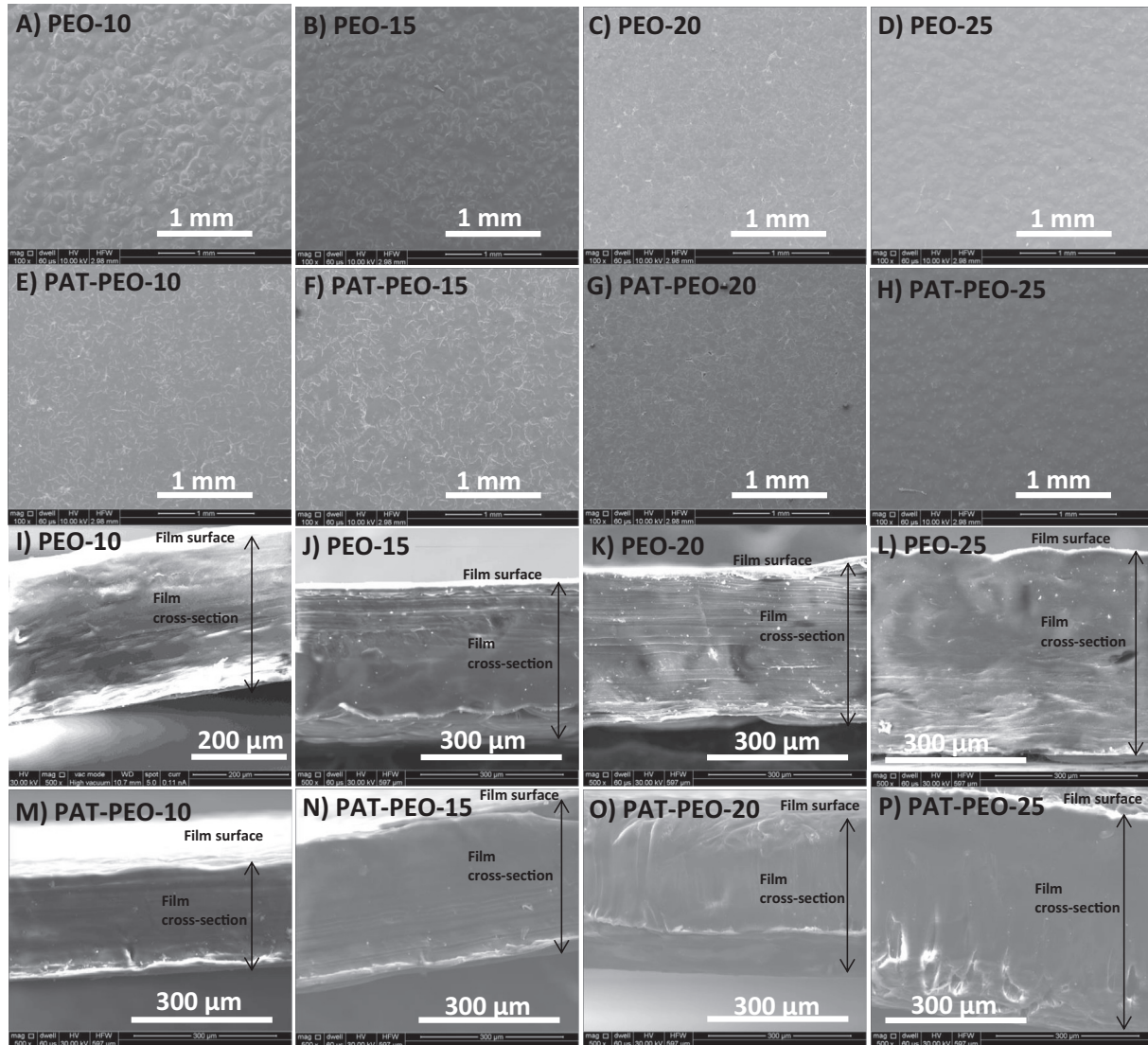


Fig. 2. SEM images of surfaces (A–H) and cross-sections (I–P) of control PEO films and PAT-PEO films.

2–3 $\mu\text{g}/\text{mm}^2$ was effective in successfully inhibiting restenosis in patients with peripheral vascular disease [12,24,25]. Based on these literature, the doses of PAT released from PAT-PEO films prepared in this study are clinically relevant for inhibiting restenosis.

3.2. SEM characterization of control PEO and PAT-PEO films

Fig. 2 shows the SEM images of surfaces and cross-sections of control PEO and PAT-PEO films prepared in this study. The surfaces of both the control PEO and PAT-PEO films were homogenous with small fissures present on the surfaces (Fig. 2A–H). Also, all PAT-PEO film surfaces (Fig. 2E–H) appeared smoother than their corresponding control PEO film surfaces (Fig. 2A–D). The cross-sections of control and PAT-PEO films were also homogenous (Fig. 2I–P). Using SEM cross-sectional images, the thickness of PEO-10, PEO-15, PEO-20, PEO-25, PAT-PEO-10, PAT-PEO-15, PAT-PEO-20, and PAT-PEO-25 films was determined as $263 \pm 64 \mu\text{m}$, $342 \pm 74 \mu\text{m}$, $445 \pm 77 \mu\text{m}$, $517 \pm 45 \mu\text{m}$, $200 \pm 43 \mu\text{m}$, $322 \pm 36 \mu\text{m}$, $413 \pm 18 \mu\text{m}$, and $495 \pm 26 \mu\text{m}$, respectively. Similar to the surface, the cross-sections of PAT-PEO films (Fig. 2M–P) were smoother than that of their corresponding control PEO films (Fig. 2I–L). This could suggest that the PAT acted as a filler by bridging the space between PEO polymeric chains to

smoothen the PAT-PEO films. Also, no PAT crystals were present on the surface of PAT-PEO films (Fig. 2E–H). This suggested that the PAT was successfully incorporated into the bulk of PEO films. The cross-sections of PAT-PEO films also did not show the presence of PAT crystals (Fig. 2M–P). This suggested that the PAT was molecularly dispersed in PEO with no crystals formed inside the films irrespective of the type of PAT-PEO films prepared in this study.

3.3. OSP characterization of control PEO and PAT-PEO films

Fig. 3 shows the 3D OSP topography images of control and PAT-PEO films. These images show how the PEO crystals were distributed on the films. For the PEO-10 and PEO-15 films, the crystals were loosely scattered with some crystals merging together. However, for the PEO-20 and PEO-25 films, the crystals were densely packed with many of them merging together. For the PAT-PEO-10 and PAT-PEO-15 films, the crystals were denser than that of their corresponding control PEO films. For the PAT-PEO-20 and PAT-PEO-25 films, the crystals were larger and denser than that of their corresponding control PEO films. Table 1D shows the average surface roughness (S_a) of control PEO and PAT-PEO films. Irrespective of control PEO or PAT-PEO films, the surface

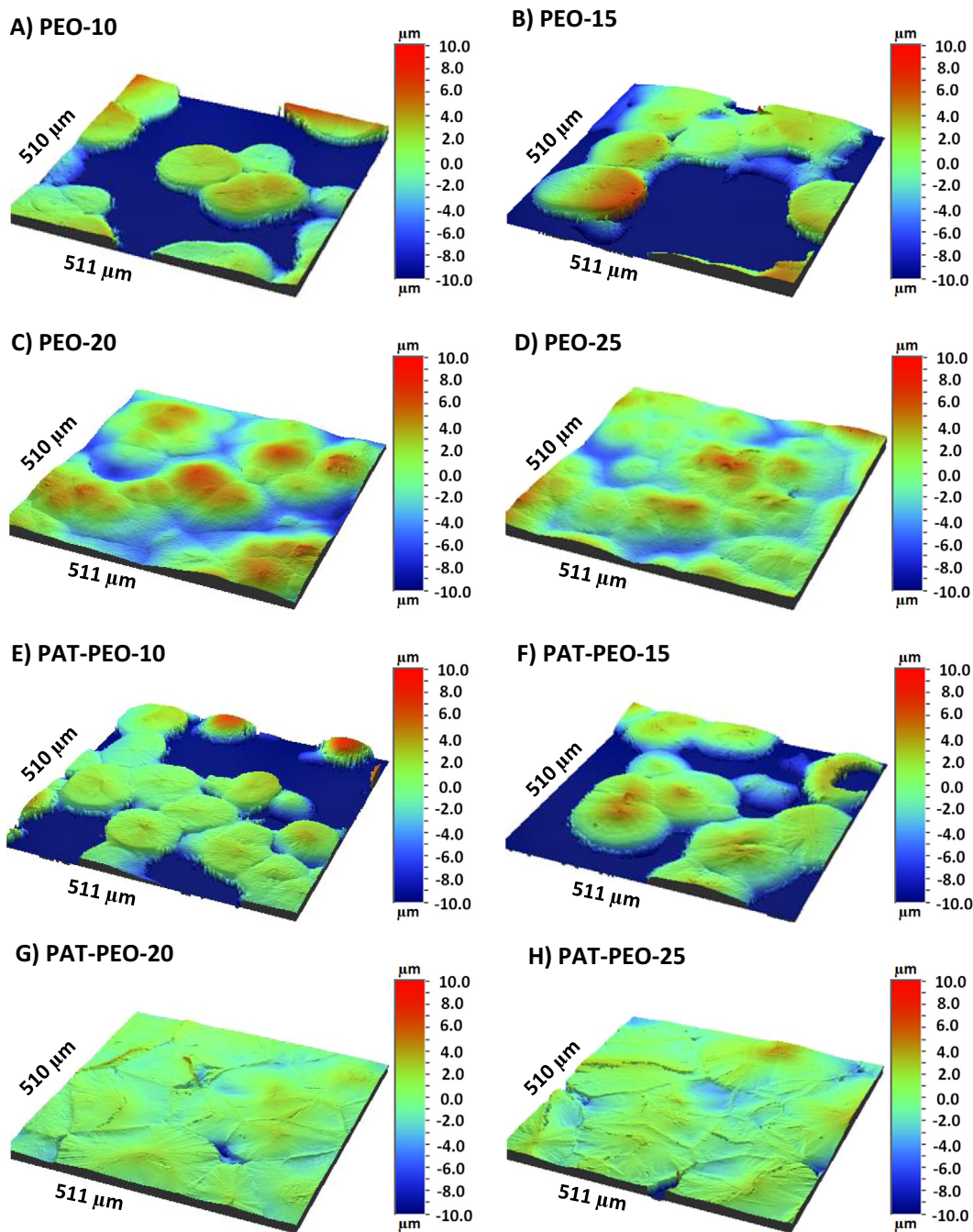


Fig. 3. 3D optical surface profilometry images of control PEO films and PAT-PEO film surfaces.

Table 1D

Average surface roughness (S_a) of control PEO films and PAT-PEO films measured at $511 \mu\text{m} \times 510 \mu\text{m}$ field of view.

Sample group	S_a (μm)
PEO-10	10.3 ± 2.8
PEO-15	11.2 ± 3.0
PEO-20	2.7 ± 0.3
PEO-25	2.3 ± 0.6
PAT-PEO-10	9.1 ± 2.4
PAT-PEO-15	9.3 ± 0.6
PAT-PEO-20	0.9 ± 0.1
PAT-PEO-25	1.3 ± 0.2

roughness of the films prepared with 20 and 25 w/v% of the polymer was four times lower than that of the films prepared with 10

and 15 w/v% of the polymer. This suggested that the films prepared with higher w/v% (20 and 25) are smoother than that of the films prepared with lower w/v% (10 and 15). Also, the surface roughness of PAT-PEO films was lower than that of their corresponding control-PEO films especially when the films were prepared with higher w/v% (20 and 25). This result further emphasizes that the addition of PAT improves the smoothness of the films.

3.4. FTIR characterization of control PEO and PAT-PEO films

Fig. 4A shows the FTIR spectra of PEO and PAT in powder forms. For the PEO powder (Fig. 4A-1), a large peak observed at 2878 cm^{-1} was assigned for the C-H stretching of methylene groups in the polymer. The peaks for scissoring, wagging, twisting, and rocking

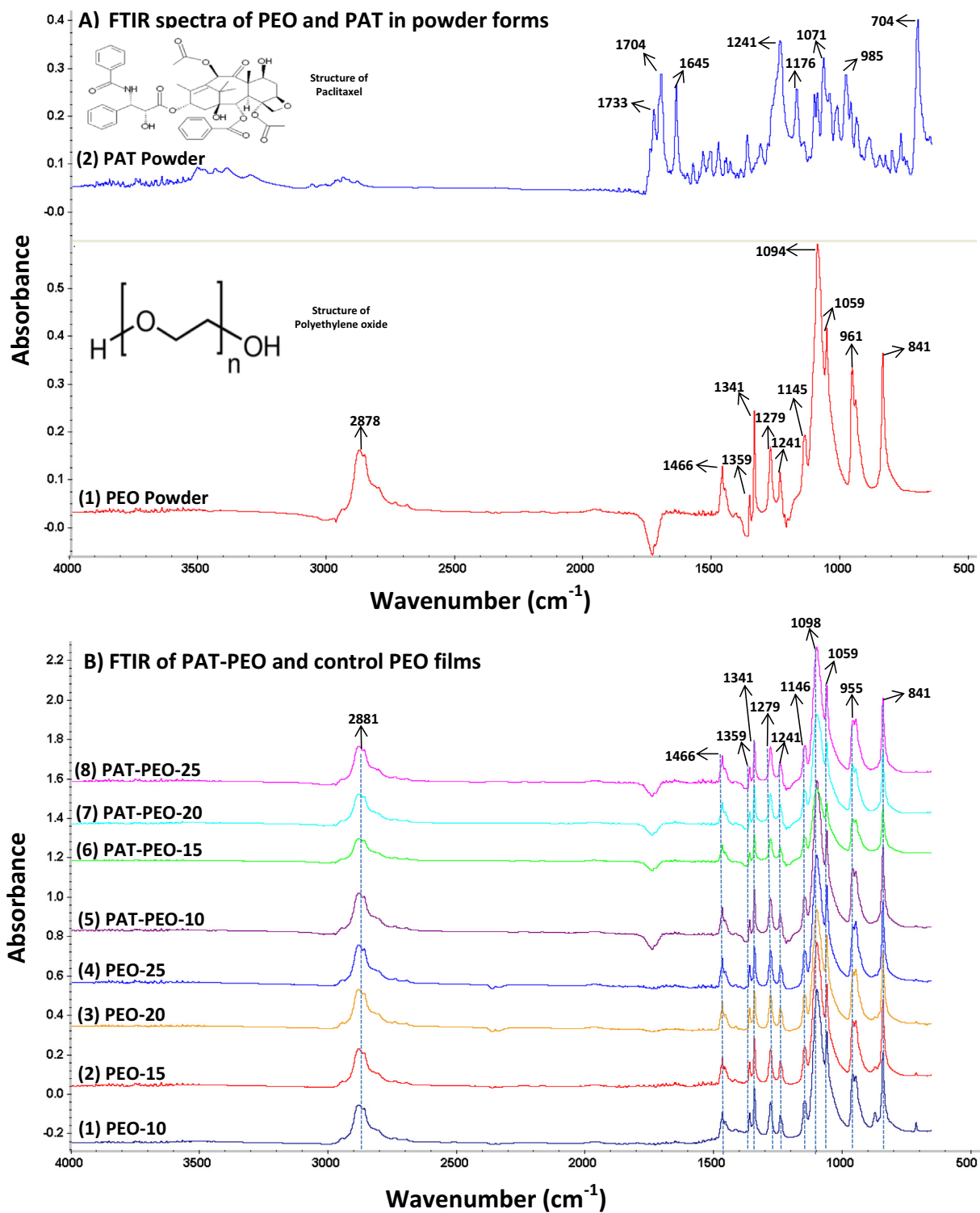


Fig. 4. FTIR spectra of PEO and PAT in powder forms (A), and control PEO films and PAT-PEO films (B).

modes of $-\text{CH}_2$ groups were observed at 1466 cm^{-1} , 1359 and 1341 cm^{-1} , 1279 and 1241 cm^{-1} , and 961 and 841 cm^{-1} , respectively. The three peaks observed at 1145 , 1094 , and 1059 cm^{-1} were assigned for the C–O–C stretches of PEO. For the PAT powder (Fig. 4A-2), the strong peaks for the C=O functionality of ester, ketone, and amide groups were observed at positions 1733 , 1704 , and 1645 cm^{-1} , respectively. Also, the peaks for the fingerprint region of PAT were observed at 1241 , 1176 , 1071 , 985 , and

704 cm^{-1} . The IR peaks and their positions of PEO and PAT powders are in well agreement with the literature [26–29].

Fig. 4B shows the FTIR spectra of control PEO and PAT-PEO films prepared in this study. The IR peaks and their positions observed for all PEO films (Fig. 4B1–4) prepared in this study are in excellent agreement with those of PEO powder. This indicated that the incorporation of PAT did not affect the chemical structure of PEO. Also, no IR peaks for PAT were observed in the spectra of

PAT-PEO films (Fig. 4B5–8). This is also in agreement with the SEM results (Section 3.2) that the PAT was incorporated into the bulk of PEO films and was not present on the film surfaces.

3.5. DSC characterization of control PEO and PAT-PEO films

Fig. 5A provides the DSC thermograms of PEO and PAT in powder forms. The melting point of PEO powder was observed at 69 °C (Fig. 5A-1). For PAT powder, an endothermic melting peak was observed at 221 °C, which was immediately followed by an exothermic decomposition peak at 231 °C (Fig. 5A-2). For the control PEO films (Fig. 5B) and PAT-PEO films (Fig. 5C), there was no significant shift in the melting point of PEO. This suggested that the crystallinity of PEO was not affected either when the polymer was made into a film or after the drug was incorporated into the polymer film. Also, no peak for PAT was observed in any of the PAT-PEO films. This is because of the less weight percentages of drug loaded (1.5%, 1%, 0.75%, and 0.6%) in the polymer. Previous studies have shown that the DSC peak for the drug loaded in the polymer was absent when the wt% of drug loaded was lesser than 5% [30].

3.6. Mechanical properties

Fig. 6 shows the stress-strain curves of control PEO and PAT-PEO films prepared in this study. Elastic modulus is the measure of stiffness or rigidity of a material. A stiff material has a high elastic modulus while a flexible material has a low elastic modulus. In this study, after the incorporation of PAT in PEO, the PAT-PEO-10 had a 23% higher elastic modulus than that of control PEO-10 (Table 1E). However, PAT-PEO-15, 20, and 25 had a 10%, 29%, and 21% smaller elastic modulus than that of control PEO-15, 20,

and 25, respectively. These results suggested that the incorporation of drug in PEO increases the flexibility of films except for the films prepared with 10 w/v% of polymer. Strain at break is the measure of ductility of materials. PAT-PEO-10, 15, 20, and 25 films showed 140%, 29%, 74%, and 62% increased strain at break when compared to their corresponding control PEO films (Table 1E). This suggested that the incorporation of drug makes the films more ductile. The peak load is directly related to yield strength, which determines how much stress a sample can withstand before it plastically deforms. The peak load for PAT-PEO-10 was significantly greater (53%) than that of PEO-10 (Table 1E). However, for the films prepared with 15, 20, and 25 w/v% of polymer, no significant difference in peak load was observed between control PEO and PAT-PEO. These results suggested that the incorporation of drug did not negatively affect the yield strength of the material. Tensile strength is the maximum amount of stress that a material can withstand before breaking. Hence, the greater the tensile strength, the stronger the material. The tensile strength for PAT-PEO-10 was significantly greater (97%) than that of PEO-10 (Table 1E). This suggested PAT-PEO-10 was stronger than PEO-10. However, for the films prepared with 15, 20, and 25 w/v% of polymer, no significant difference in tensile strength was observed between control PEO and PAT-PEO. These results suggested that the incorporation of drug did not negatively affect the strength of the films.

3.7. Characterization of PAT-PEO films post drug-elution study

The FTIR characterization of PAT-PEO-10, PAT-PEO-15, PAT-PEO-20, and PAT-PEO-25 films collected after 1 min, 2.5 min, 3.15 min, and 6 min of drug-elution studies, respectively, are provided in Fig. 7A. The peaks for the different functionalities

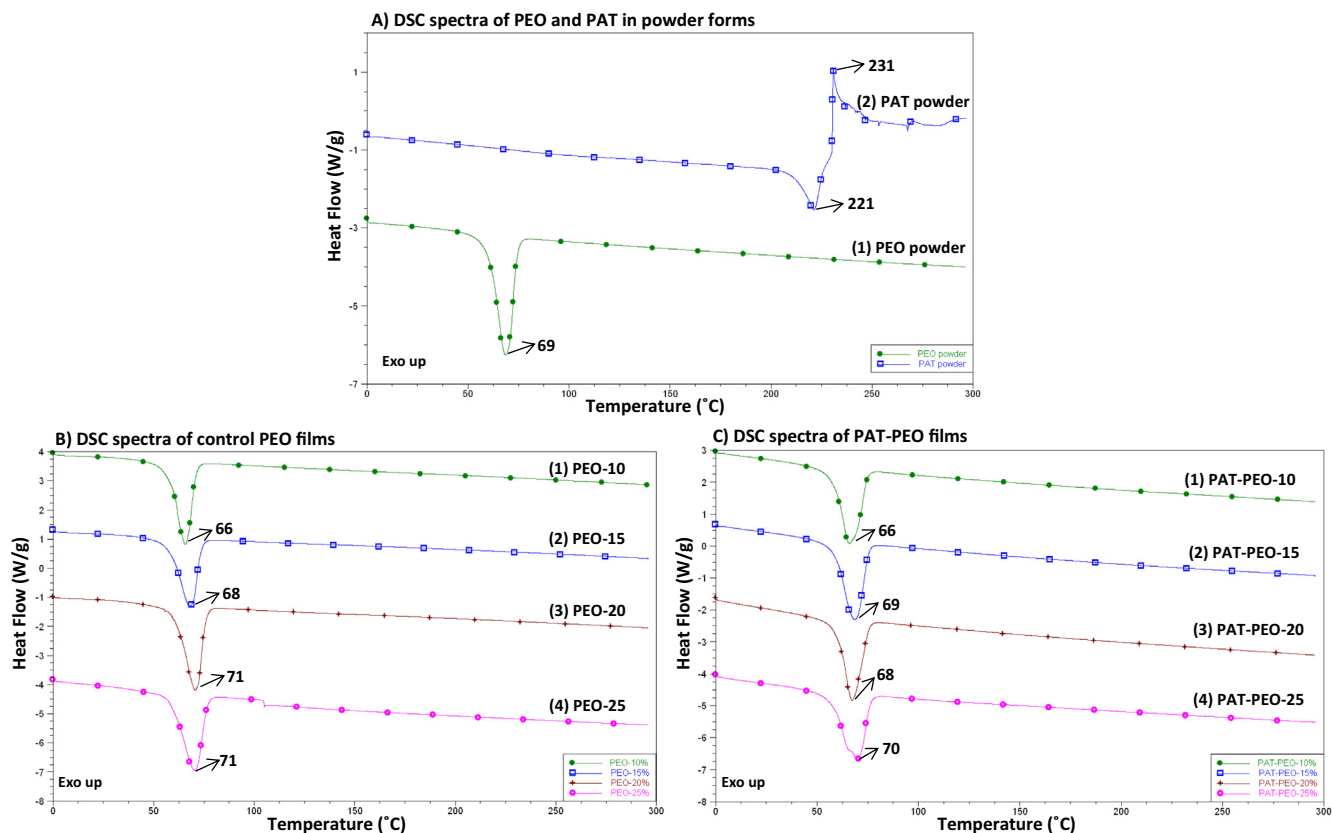


Fig. 5. DSC spectra of PEO and PAT in powder forms (A), control PEO films (B), and PAT-PEO films (C).

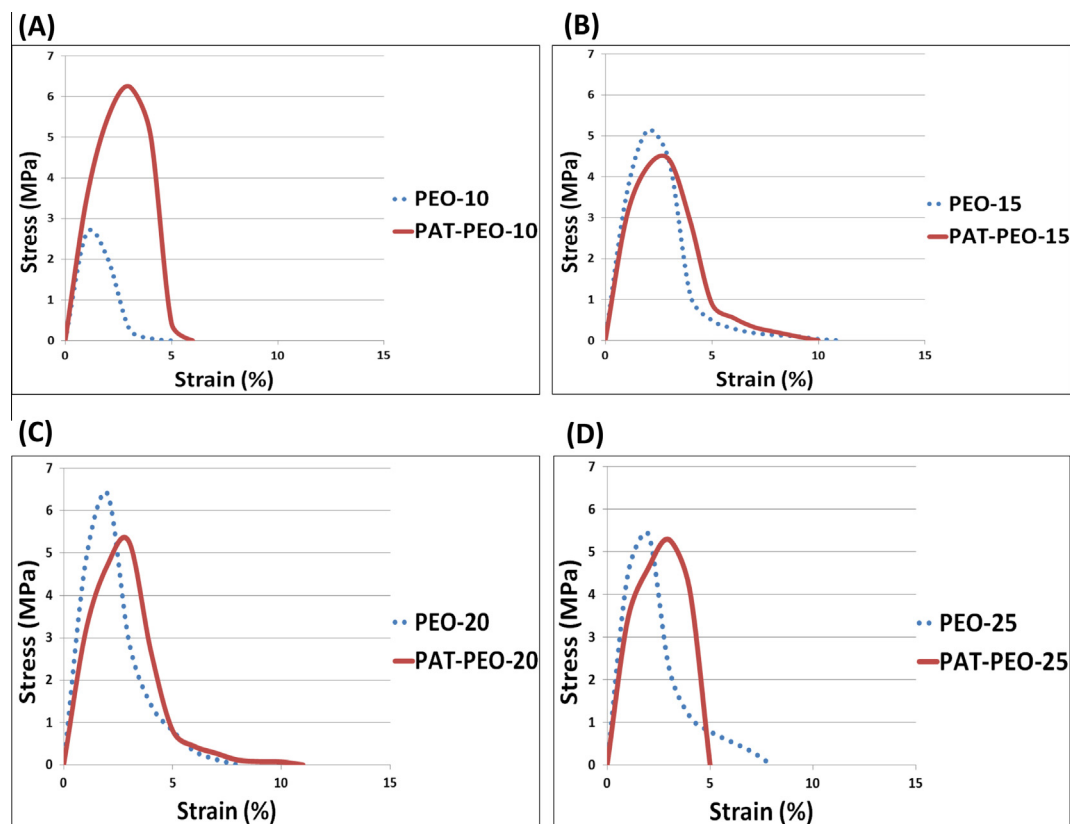


Fig. 6. Stress–strain curves of PEO-10 and PAT-PEO-10 (A), PEO-15 and PAT-PEO-15 (B), PEO-20 and PAT-PEO-20 (C), and PEO-25 and PAT-PEO-25 (D).

Table 1E

Mechanical properties of control PEO films and PAT-PEO films.

Sample group	Elastic modulus (MPa)	Strain at break (%)	Peak load (lbf)	Tensile strength (MPa)
PEO-10	279 ± 21	1.5 ± 0.1	1.9 ± 0.2	3.3 ± 0.4
PEO-15	399 ± 39	2.4 ± 0.2	4.1 ± 0.5	5.3 ± 0.7
PEO-20	527 ± 72	1.9 ± 0.3	6.5 ± 1.2	6.5 ± 1.2
PEO-25	541 ± 43	2.1 ± 0.5	6.4 ± 0.1	5.5 ± 0.1
PAT-PEO-10	342 ± 34	3.6 ± 0.6	2.9 ± 0.4	6.5 ± 0.9
PAT-PEO-15	358 ± 49	3.1 ± 0.8	3.4 ± 0.4	4.7 ± 0.6
PAT-PEO-20	373 ± 46	3.3 ± 0.1	5.0 ± 0.8	5.3 ± 0.8
PAT-PEO-25	426 ± 58	3.4 ± 0.4	6.0 ± 0.8	5.4 ± 0.7

of PEO such as C–H (2918 cm^{-1}), $-\text{CH}_2$ (1457 , 1355 , 1245 , and 948 cm^{-1}), and C–O–C (1081 cm^{-1}) were observed. This shows that the chemical structure of PEO molecules was not altered in the specimens (loose disintegrated films) collected after drug-elution studies. These results suggested that the drug release from PAT-PEO films occurred due to dissolution of films and not due to biodegradation of polymer. A broad peak observed at 3370 cm^{-1} was due to H_2O molecules absorbed in the films during its immersion in PBS/T-20 solution. Also, the peaks observed at 1645 cm^{-1} and 1733 cm^{-1} were assigned to the C=O functionality of amide and ester groups of PAT delivered from the films, respectively. Fig. 7B shows the DSC thermograms of PAT-PEO films collected after the drug-elution studies. The thermograms showed two peaks between $100\text{ }^\circ\text{C}$ and $125\text{ }^\circ\text{C}$ due to evaporation of free and bonded water from the films. However, no melting peak for the PEO crystals was observed at $65\text{--}70\text{ }^\circ\text{C}$. This strongly suggested that all PEO crystals were disintegrated under the conditions used for drug-elution studies. These results further emphasized that the drug was delivered from the PAT-PEO films due to dissolution of films. Fig. 7C shows the real-time images of PAT-PEO films obtained using phase contrast microscopy at different time points.

Prior to its immersion in PBS/T-20, the films were intact as it appeared mostly dark. The films absorbed most of the light and reflected little to appear mostly dark. However, after immersion in PBS/T-20, the PAT-PEO-10, 15, 20, and 25 films disintegrated at 2, 3, 5, and 7 min, respectively, as it is evident from the images which were mostly bright. The disintegrated films absorbed very little light to appear mostly bright. Thus, these results were in excellent agreement with FTIR and DSC to suggest that the drug was delivered from PAT-PEO films mainly due to dissolution of films.

3.8. Cell viability and proliferation

The viability and proliferation of SMCs treated with control PEO films, PAT-PEO films, and no films (control wells) are provided in Fig. 8. The cells in the control well containing no films proliferated profusely from one time point to the other. It was interesting to observe that all of the control PEO films significantly inhibited (64–76% decrease) the growth of SMCs compared to that of control wells. Also, for the control PEO films, an increase in the inhibitory effect was observed as the w/v% of PEO increased. This suggested

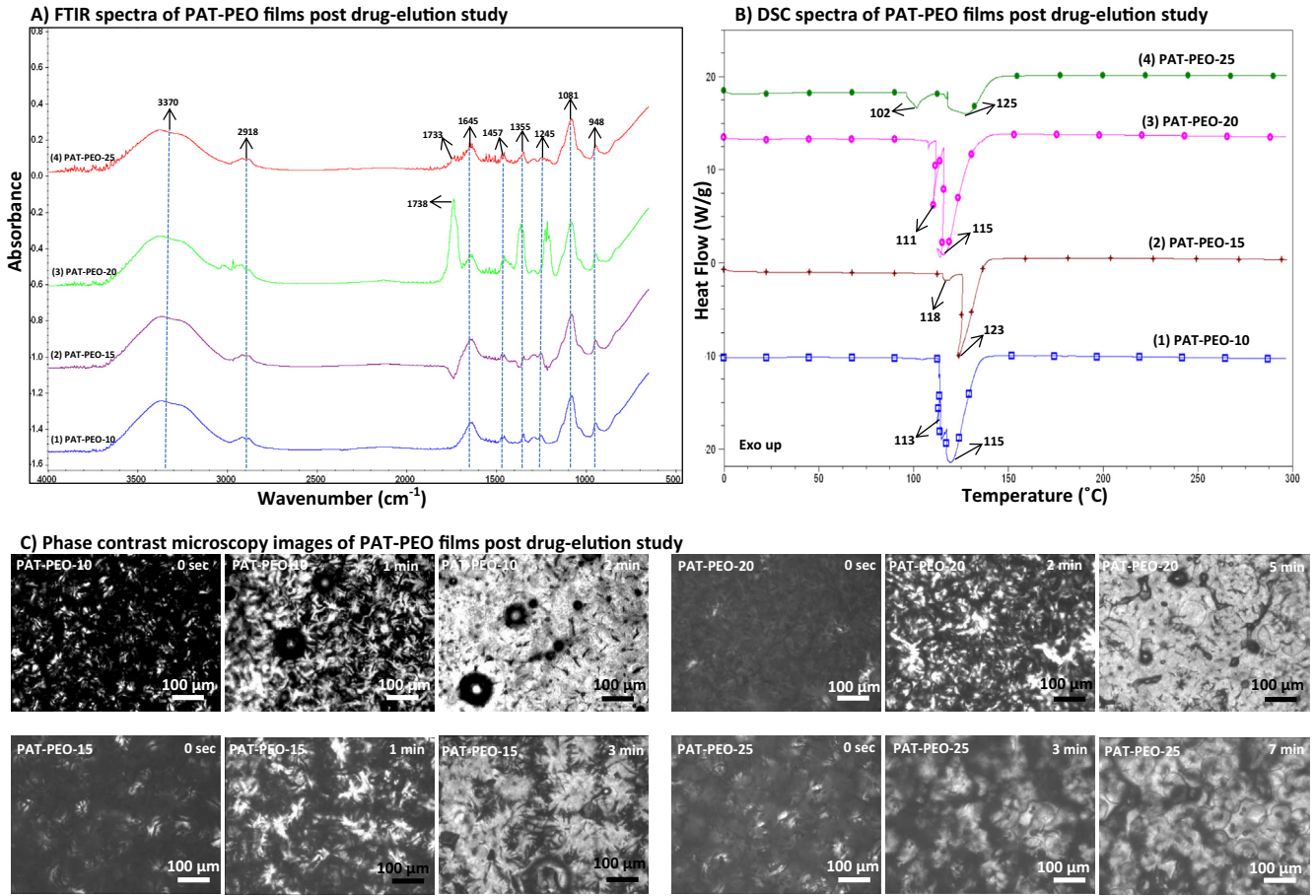


Fig. 7. FTIR spectra (A), DSC spectra (B), and phase contrast microscopy images (C) of PAT-PEO films post drug-elution study.

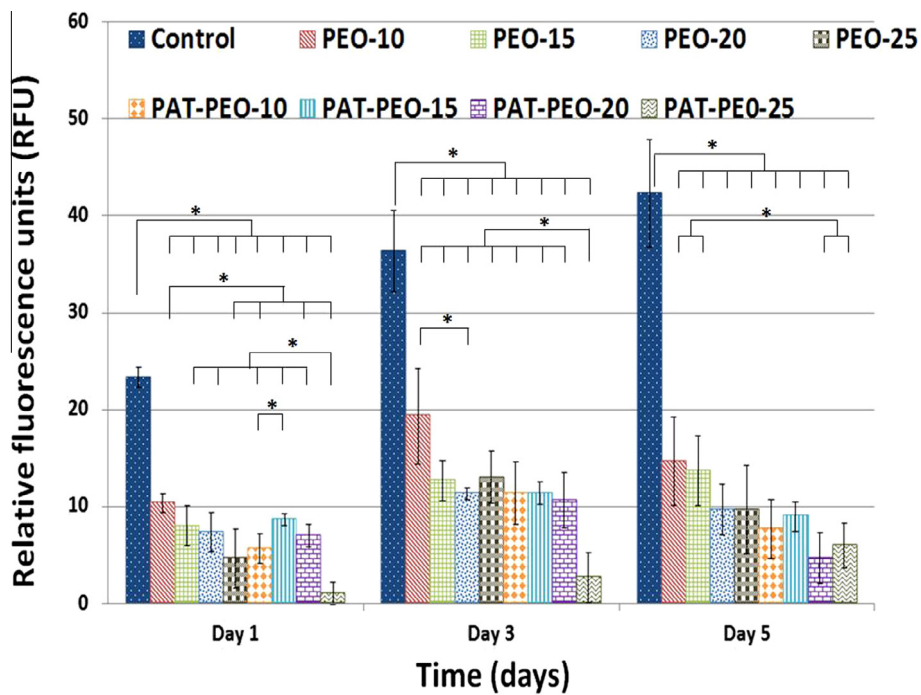


Fig. 8. Viability and proliferation of human aortic smooth muscle cells for control wells (no films), control PEO films, and PAT-PEO films.

that the PEO alone (without the drug) can significantly inhibit the growth of SMCs with greater inhibition rate observed for the films with larger w/v% of the polymer. For PAT-PEO, all films significantly inhibited (79–86% decrease) the growth of SMCs when compared to that of the control well. Also, most of the PAT-PEO films showed greater inhibitory effect (35–50% decrease) than their corresponding control PEO films (day-5 in Fig. 8).

Although the wt% of drug was lesser (0.6%) in PAT-PEO-25, these films showed maximum inhibitory effect when compared to that of all other films prepared in this study. This could be due to the combined effect of larger w/v% of polymer and the presence of drug. Thus, these results demonstrated that the PAT-PEO films prepared in this study effectively inhibited the growth of smooth muscle cells.

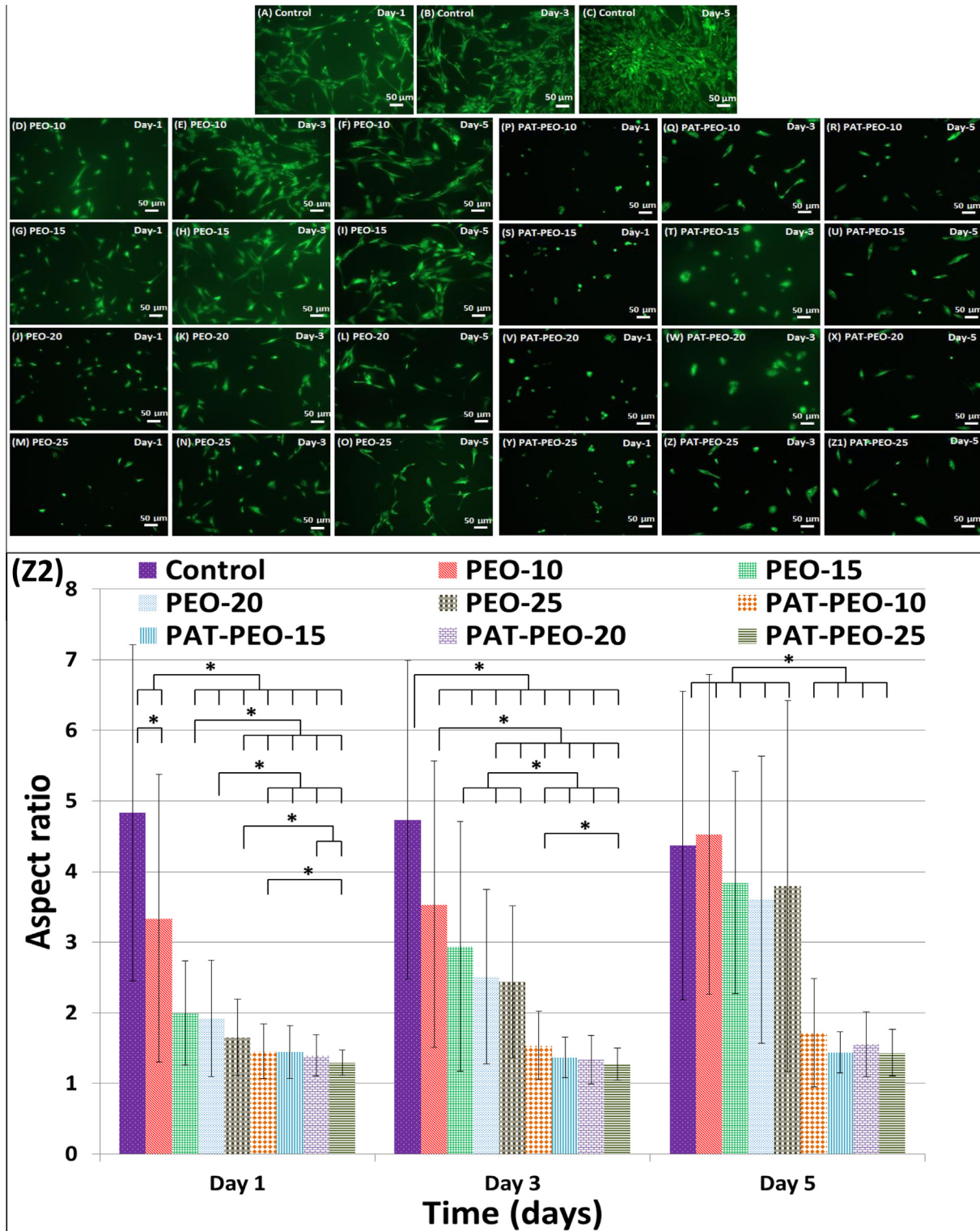


Fig. 9. Fluorescence microscopy images (A-Z1) and aspect ratio (Z2) of human aortic smooth muscle cells for control wells (no films), control PEO films, and PAT-PEO films.

3.9. Cell morphology

Fig. 9 shows the fluorescent microscopy images of the FDA stained SMCs treated with control PEO films, PAT-PEO films, and no films (control wells) at days 1, 3, and 5. In the control well, the SMCs were elongated with its characteristic spindle-shape and hill-and-valley morphology (Fig. 9A–C). The cells treated with control PEO films mostly showed an irregular morphology on day-1 (Fig. 9D,G,J,M). However, by day-5, the cells treated with control PEO films started to show the normal spindle-shaped morphology (Fig. 9F,I,L,O). This could suggest that PEO alone may not provide the long-term inhibitory effect. Hence, the incorporation of anti-proliferative agents is crucial for providing long-term inhibitory effect to these films. Also, an increasing number of normal spindle-shaped cells were observed for the films prepared with lower w/v% (10 and 15) of polymer (Fig. 9F and I) than the films prepared with higher w/v% (20 and 25) of polymer (Fig. 9L and

O). This further emphasizes that higher w/v% of polymer has greater inhibitory effect on SMCs. For all PAT-PEO films (Fig. 9P–Z1), the cells displayed an uncharacteristic discoid (flat circular) morphology for all time points used in this study. After 5 days, the confluency of SMCs in the control well, control PEO-10, 15, 20, and 25 films were estimated as 90–95%, 50–60%, 50–60%, 20–25%, and 20–25%, respectively. For all four PAT-PEO groups, very few viable cells were only observed after day-5 with <10% confluency. These qualitative data are in excellent agreement with the quantitative results described in the previous paragraph (Section 3.8). The aspect ratio of SMCs treated with control PEO films, PAT-PEO films, and no films (controls) are shown in Fig. 9Z2. On day-1, the aspect ratio of the cells treated with PAT-PEO films (1.3–1.5) and most PEO films (1.7–2.0 for PEO-15, 20, and 25) are twice smaller than that of the controls (5.0 ± 2.0). The range of aspect ratio of the cells in controls remained same for up to day-5. Similarly, the range of aspect ratio of the cells treated with

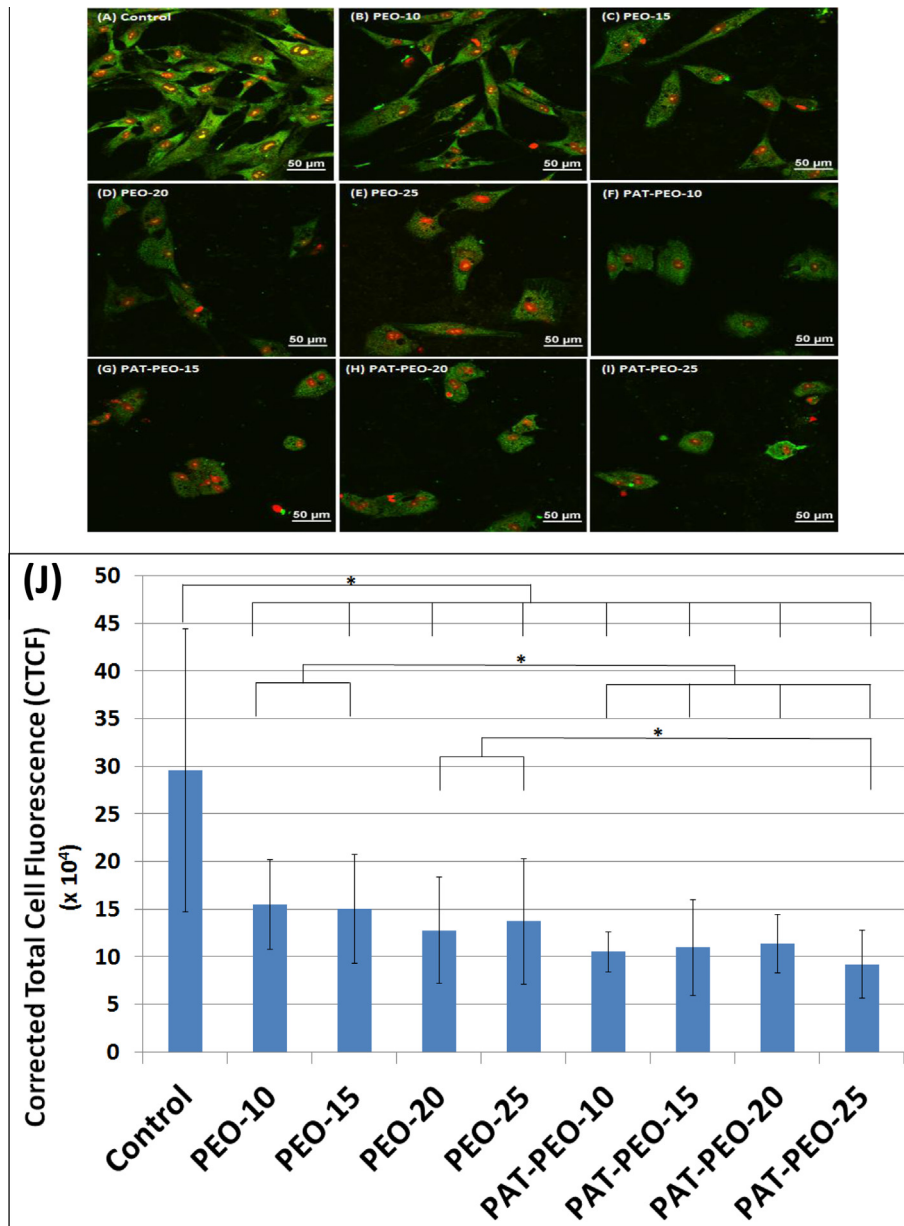


Fig. 10. Immunofluorescent microscopy images (A–I) and smooth muscle α -actin quantification (J) of human aortic smooth muscle cells for control wells (no films), control PEO films, and PAT-PEO films.

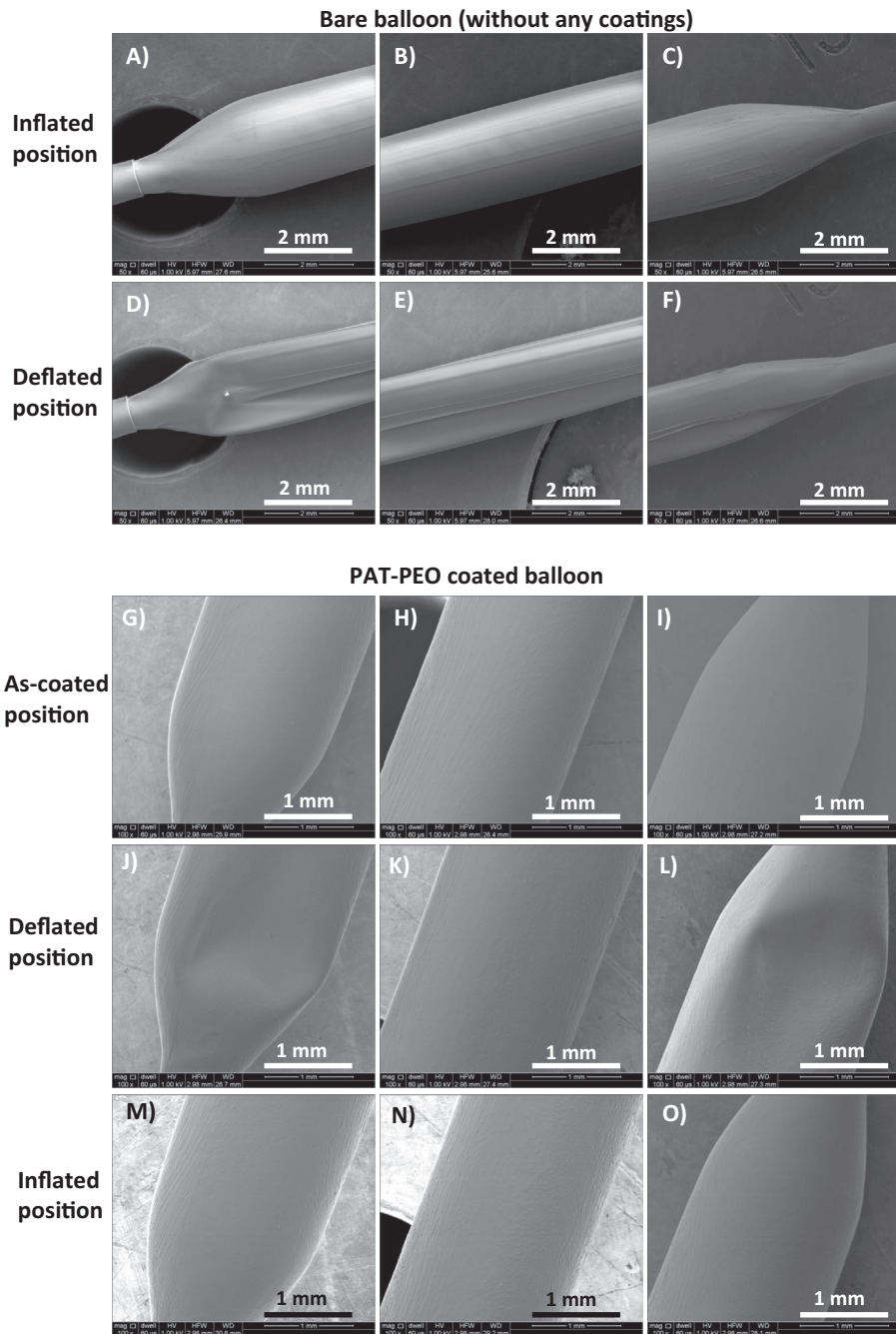


Fig. 11. SEM images of bare balloon (A–F) and PAT–PEO coated balloon (G–O).

PAT–PEO films remained same for up to day-5. However, the cells treated with control PEO films showed an increase in aspect ratio from day-1 to day-5. On day-5, there was no significant difference observed in the aspect ratio of cells treated with control PEO films and controls.

3.10. Cell phenotype

Smooth muscle (SM) α -actin is a cytoskeletal protein that is primarily responsible for the motility, structure, and integrity of SMCs [31]. A strong expression of SM α -actin is usually observed for well growing SMCs [20]. Also, the α -actin filaments orient along the cell axis in well growing SMCs. However, when the cells are damaged, the expression of SM α -actin will be poor [20]. Also, the α -actin filaments are typically disarranged in damaged SMCs. In this study,

the immunofluorescence microscopy images of SMCs treated with control PEO, PAT–PEO, and no films (control wells) are provided in Fig. 10. The cells in the control well showed a stronger SM α -actin expression (intense staining) with the α -actin filaments oriented along the cell axis (Fig. 10A). This suggested the healthy state of SMCs in control wells. However, the SM α -actin expression was weaker (less intense staining) for all control PEO films (Fig. 10B–E). Also, the cells showed a disarrangement of actin filaments with an irregular orientation (Fig. 10B–E). This result showed the inhibitory effect of control PEO films on SMC growth. For PAT–PEO films, only very few cells showed the expression of SM α -actin (Fig. 10F–I). Also, the expression was very weak with α -actin filaments disarranged in circumferential orientation. This result strongly suggested that PAT–PEO films effectively inhibited the growth of SMCs. The quantification of smooth muscle α -actin

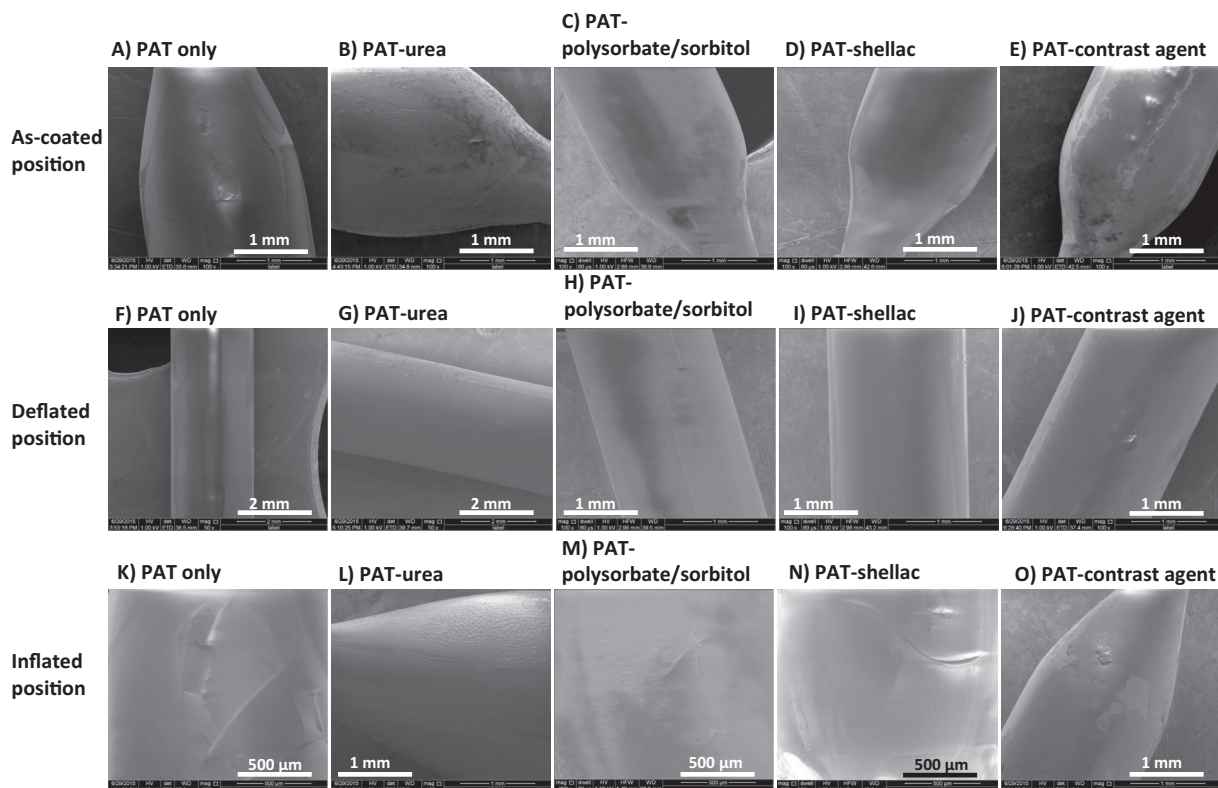


Fig. 12. SEM images of control drug-coated balloons prepared using PAT only (A, F, K), PAT-urea (B, G, L), PAT-polysorbate/sorbitol (C, H, M), PAT-shellac (D, I, N), and PAT-iodixanol (E, J, O).

for the controls and all treatment groups are provided in Fig. 10J. The expression of SM α -actin in the cells treated with control PEO films and PAT-PEO films was decreased by half when compared to that of controls. No significant difference in the SM α -actin was observed between the different groups of control PEO films or PAT-PEO films. However, the expression observed for all PAT-PEO films was significantly lesser than that of PEO-10 and PEO-15. Also, expression for PAT-PEO-25 was significantly lesser than that of PEO-20 and PEO-25 as well. These results are in agreement with the literature as PAT has been shown to significantly decrease the expression of SM α -actin [32,33].

3.11. PAT-PEO coatings on balloons

Fig. 11A–C and D–F shows the SEM images of bare balloons (without any coatings) in inflated and deflated positions, respectively. These images show that the balloons were fully expanded in its inflated position and were showing flaps in its deflated position. Fig. 11G–I, J–L, and M–O shows the SEM images of PAT-PEO coated balloons in as-coated, deflated, and inflated positions, respectively. These images showed that the PAT-PEO coating was smooth, uniform, and homogeneous on the balloon surface (Fig. 11G–I). Also, the integrity of PAT-PEO coating on the balloons was well maintained without any mechanical defects occurring during inflation or deflation (Fig. 11J–O).

3.12. Currently available drug-carrier combination coatings on balloons

Fig. 12A–E, F–J, and K–O shows the SEM images of control DCBs prepared using currently available drug-carrier combinations in as-coated, inflated, and deflated positions, respectively. These images showed that these coatings are not smooth, nonuniform, and inhomogeneous at several different spots on the balloon

(Fig. 12A–E). Also, these coatings undergo mechanical defects during balloon inflation or deflation to produce irregularities, ridges, cracks, fissures, and rough textures (Fig. 12F–O).

3.13. Drug release from PAT-PEO coating on balloon

For treatments using DCBs, the typical balloon tracking time is from 30 s to 1 min. Once the balloon reaches the diseased site, a time frame of 2–3 min is recommended for the treatment including balloon inflation and drug delivery [24]. Hence, in this study, we have considered the initial 1 min time as the typical time period for balloon tracking, and the following 3 min (from 1 min to 4 min) as the typical time period for treatment including inflation and drug delivery. The total amount of PAT loaded on the PAT-PEO coated balloons is $2.23 \pm 0.31 \mu\text{g}/\text{mm}^2$. The currently available DCBs carry drug doses in the range of $2 \mu\text{g}/\text{mm}^2$ to $3 \mu\text{g}/\text{mm}^2$ [24]. Hence, the total amount of PAT loaded on the balloons using the PEO platform is clinically relevant for controlling neointimal hyperplasia. The cumulative amount and percentage of PAT release from PAT-PEO coatings are provided in Figs. 13A and 14A, respectively. Only 15% of the total PAT loaded was released from the balloons during the initial 1 min (typical balloon tracking time) whereas 80% of the drug was released during 1 min to 4 min (typical treatment time period) and only 5% of the drug was present on the balloons after 4 min as a residual drug.

3.14. Drug release from currently available drug-carrier combination coatings on balloons

The total amount of PAT loaded on the balloons using currently available drug-carrier combination coatings such as PAT only, PAT-urea, PAT-polysorbate/sorbitol, PAT-shellac, and PAT-contrast agent is 0.17 ± 0.11 , 0.11 ± 0.03 , 0.03 ± 0.01 , 0.09 ± 0.02 , and $0.05 \pm 0.4 \mu\text{g}/\text{mm}^2$, respectively. The cumulative release and

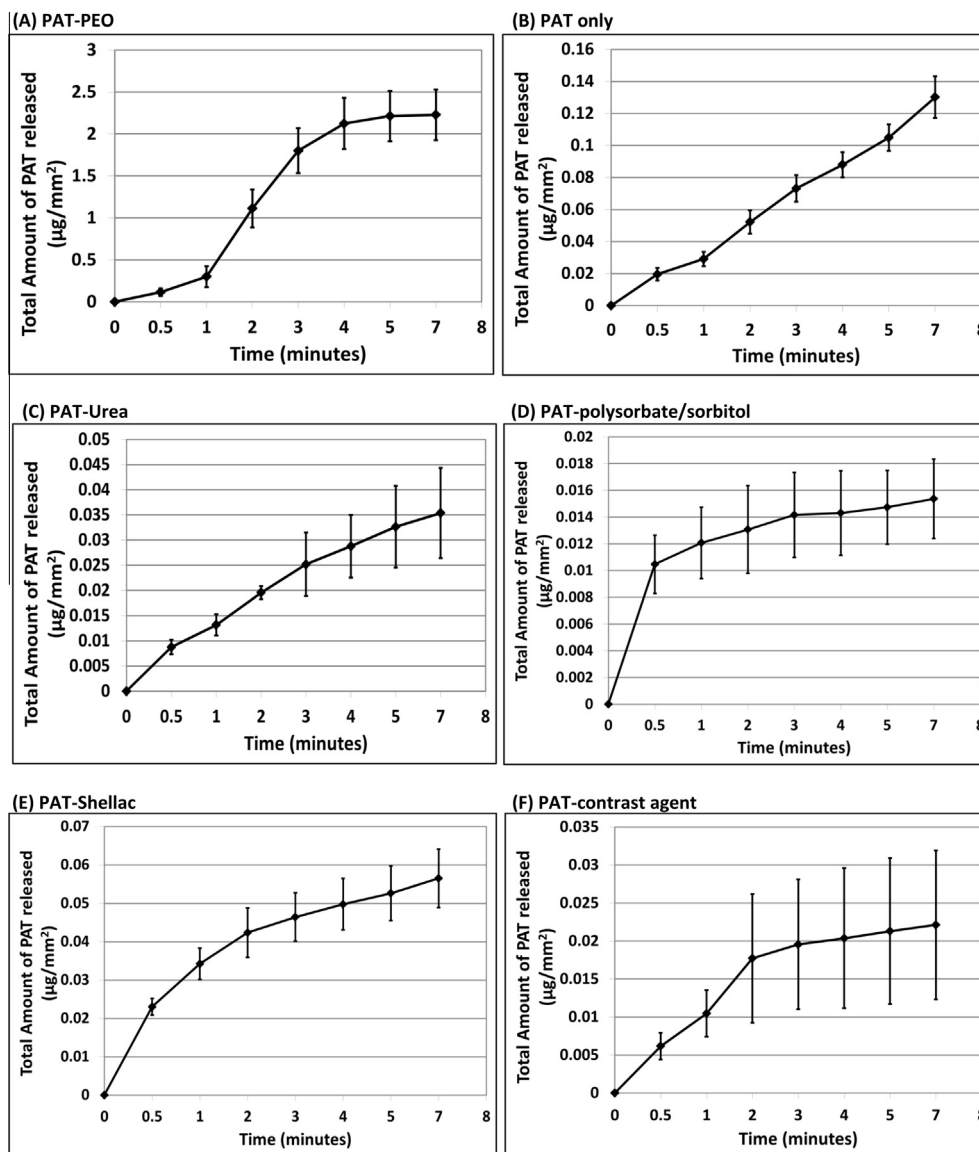


Fig. 13. Cumulative PAT released ($\mu\text{g}/\text{mm}^2$) from PAT-PEO coated balloons (A) and control drug-coated balloons (B-F).

percentage of PAT release from these coatings are provided in Fig. 13B–F and Fig. 14B–F, respectively. PAT only control showed that only 26% of the total PAT loaded was released between 1 min and 4 min while 13% of the drug was released during the initial 1 min and 61% of the drug was retained on the balloon after 4 min. For PAT-urea, only 15% of the total drug loaded was released between 1 min and 4 min while 13% was released during the initial 1 min and 72% was retained on the balloon after 4 min. For PAT-polysorbate/sorbitol, only 7% of the total drug loaded was released between 1 min and 4 min while 36% was released during the initial 1 min and 58% was retained on the balloon after 4 min. For PAT-shellac, only 18% of the total drug loaded was released between 1 min and 4 min while 40% was released during the initial 1 min and 42% was retained on the balloon after 4 min. For PAT-contrast agent, only 24% of the total drug loaded was released between 1 min and 4 min while 32% was released during the initial 1 min and 43% was retained on the balloon after 4 min.

4. Discussion

In this study, we have explored the use of polyethylene oxide (PEO) films for applications in DCBs. PEO is a biocompatible

polymer approved by U.S. Food and Drug Administration (FDA) for internal use by humans [34]. PEO is used as an excipient in a variety of pharmaceutical products that are administered orally and parenterally in humans [34]. PEO is not a biodegradable polymer. The half-life of PEO in blood circulation ranges from 18 min to 1 day as its molecular weight increased from 6000 to 190,000 [35]. The excretion of PEO from the body depends on its molecular weight. The lower molecular weight PEO have been primarily excreted through urine while the higher molecular weight (>50,000) PEO have been excreted through feces [35]. Due to all these significant advantages, PEO has been extensively used for drug delivery applications.

PEO used for drug delivery is either uncrosslinked or crosslinked depending on the applications [36,37]. The pure uncrosslinked PEO is typically used in pharmaceutical products such as oral tablets, bioadhesives, and osmotic pump tablets, while the crosslinked PEO networks are used for applications in implants and medical devices [36,37]. The reason that pure uncrosslinked PEO is not commonly used in implants and medical devices is that the polymer dissolves very quickly in water-based solutions. Therefore, it is not possible to use this system for delivering drugs for an extended period of time, which is the norm in most

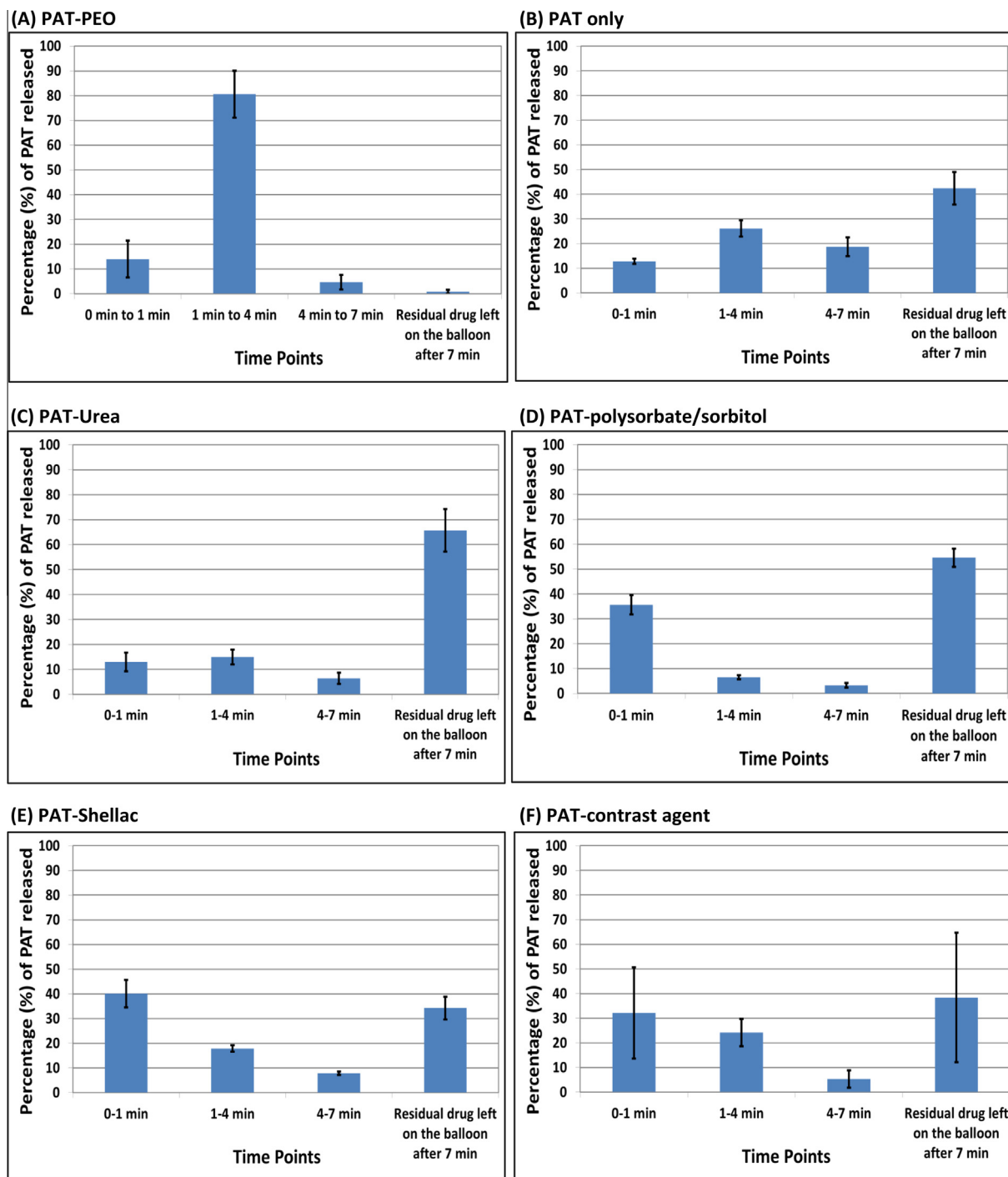


Fig. 14. Percentage of PAT released from PAT-PEO coated balloons (A) and control drug-coated balloons (B-F).

drug-eluting medical devices. It is this quick dissolution property that makes the uncrosslinked PEO a promising material for applications in DCBs. Furthermore, the physiochemical properties of PEO can be adjusted easily by varying the w/v% of polymer to tailor the drug release at any specific time intervals between 1 min and 7 min, which is the time frame required for interventionalists to carry out any basic or advanced clinical procedures involving angioplasty as well as balloon-based drug delivery. In this study, as evident from the SEM cross-sectional imaging, the thickness (200 μm–500 μm) of the PAT-PEO films increases as the w/v% (10–25%) of the polymer increases. The thicker the film, the longer the time it takes to dissolve and slowly deliver the drug. This has

led to the delayed release of various PAT-PEO formulations prepared in this study.

The PAT-PEO coated balloons and five control DCBs were prepared using the same dip coating procedure and by keeping the same concentration of PAT in the coating solutions. SEM images showed that the PAT-PEO coating on the balloon was homogeneous and the coating integrity was well maintained without any mechanical defects occurring during balloon inflation or deflation. However, the coatings on the control DCBs were non-homogenous and different types of mechanical defects were observed when the balloons were inflated or deflated. This shows the use of PEO as a mechanically robust coating for the balloons. The amount of PAT

loaded on PAT–PEO coated balloons was 13 times, 20 times, 74 times, 24 times, and 45 times greater than the amount of PAT loaded on PAT-only, PAT–urea, PAT–polysorbate/sorbitol, PAT–shellac, and PAT–contrast agent control DCBs, respectively. This signifies the use of a polymeric carrier such as PEO in carrying an adequate amount of drug on the balloons. If a different coating procedure such as spray coating is employed, it is possible to load more amount of PAT on the control DCBs. However, the accumulation of more PAT directly on a material surface without a polymer-based drug carrier could lead to the formation of loosely bound PAT crystals to provide a burst release [17].

For DCB based therapy, a biphasic drug release profile with an initial no drug release (up to 1 min) followed by an immediate quick release of all the drug (between 1 min and 4 min) is needed. The PAT–PEO film prepared in this study provided such drug release profile with a minimal drug release (~15%) during the initial 1 min followed by an immediate quick drug release (~80%) between 1 min and 4 min. The PAT–PEO films prepared undergo controlled dissolution under physiological conditions to deliver the drug only at specific time intervals that is suitable for DCB based therapy. Such controlled dissolution property of PAT–PEO films makes it a promising coating material for DCBs. For the controls such as PAT only and PAT–urea, a sustained drug release was observed, whereas for the controls such as PAT–polysorbate/sorbitol, PAT–shellac, and PAT–contrast agent, a biphasic release profile with an initial burst release followed by a slow and sustained release was observed. Such release profiles are not suitable for DCB based therapy. The diffusion of drug from the coating and the dissolution of carriers are considered to be primary mechanisms for drug release from the controls used in this study. In this study, 80% of the PAT loaded on the PAT–PEO coated balloons was released between 1 min and 4 min (the typical time period of balloon inflation and treatment). For the same time period, the % of PAT released from PAT-only, PAT–urea, PAT–polysorbate/sorbitol, PAT–shellac, and PAT–contrast agent control DCBs were 26%, 15%, 7%, 18%, and 24%, respectively. This further demonstrates the role of PEO in controlling the delivery of drug from the balloons.

5. Conclusions

Various PAT–PEO films were developed in this study for applications in DCBs with a motivation to prevent initial drug loss during balloon tracking and then to immediately deliver most of the drug within a very short time period of balloon inflation and treatment. The w/v% of PEO and wt% of PAT were varied in PAT–PEO films to tailor the drug release in such a way that >90% of drug was released only at specific time intervals. The SEM and FTIR collectively showed that the PAT–PEO films developed were homogeneous and the PAT was molecularly dispersed in the PEO matrix. DSC showed that the crystallinity of PEO was not affected after the incorporation of PAT. The PAT–PEO films developed were flexible and ductile with no effect observed on the yield or tensile strengths of the films after drug incorporation. The FTIR, DSC, and phase contrast microscopy characterizations of PAT–PEO films post drug-elution study showed the dissolution of PEO under physiological conditions as the primary mechanism for the delivery of PAT. The cell culture studies showed that both the control PEO and PAT–PEO films successfully inhibited the growth of SMCs with a superior inhibitory effect observed for PAT–PEO films. The PAT–PEO coating produced on the balloons was homogeneous and the integrity of coating was well maintained without mechanical defects occurring during balloon inflation and deflation. The drug release studies showed that only 15% of the total PAT loaded was released from the balloons during the typical balloon tracking time

period (initial 1 min) while 80% of the PAT was released during the typical balloon treatment time period (from 1 min to 4 min), with only 5% of the PAT present on the balloon as a residual drug after 4 min. Thus, this study demonstrated the use of PEO as an alternate drug delivery platform for balloons.

References

- [1] K. Sarode, D.A. Spelber, D.L. Bhatt, A. Mohammad, A. Prasad, E.S. Brilakis, S. Banerjee, Drug delivering technology for endovascular management of infrainguinal peripheral artery disease, *JACC Cardiovasc. Interv.* 7 (8) (2014) 827–839.
- [2] C.A. Gongora, M. Shibuya, J.D. Wessler, J. McGregor, A. Tellez, Y.P. Cheng, G.B. Conditt, et al., Impact of paclitaxel dose on tissue pharmacokinetics and vascular healing A comparative drug-coated balloon study in the familial hypercholesterolemic swine model of superficial femoral in-stent restenosis, *JACC Cardiovasc. Interv.* 8 (8) (2015) 1115–1123.
- [3] D. Scheinert, S. Duda, T. Zeller, H. Krankenberg, J. Rieke, M. Bosiers, G. Tepe, et al., The LEVANT I (Lutonix Paclitaxel-coated balloon for the prevention of femoropopliteal restenosis) trial for femoropopliteal revascularization first-in-human randomized trial of low-dose drug-coated balloon versus uncoated balloon angioplasty, *JACC Cardiovasc. Interv.* 7 (1) (2014) 10–19.
- [4] F. Liistro, S. Grotti, I. Porto, P. Angioli, L. Ricci, K. Ducci, G. Falsini, et al., Drug-eluting balloon in peripheral intervention for the superficial femoral artery. The DEBATE-SFA randomized trial (drug eluting balloon in peripheral intervention for the superficial femoral artery), *JACC Cardiovasc. Interv.* 6 (12) (2013) 1295–1302.
- [5] S.K. Yazdani, E. Pacheco, M. Nakano, F. Otsuka, S. Naisbitt, F.D. Kolodgie, E. Ladich, et al., Vascular, downstream, and pharmacokinetic responses to treatment with a low dose drug-coated balloon in a swine femoral artery model, *Catheter. Cardiovasc. Interv.* 83 (1) (2014) 132–140.
- [6] V.B. Kolachalama, S.D. Pacetti, J.W. Franses, J.J. Stankus, H.Q. Zhao, T. Shazly, A. Nikanorov, et al., Mechanisms of tissue uptake and retention in zotarolimus-coated balloon therapy, *Circulation* 127 (20) (2013) 2047–2055.
- [7] W.A. Gray, J.F. Granada, Drug-coated balloons for the prevention of vascular restenosis, *Circulation* 121 (24) (2010) 2672–2680.
- [8] J.F. Granada, K. Milewski, H. Zhao, J.J. Stankus, A. Tellez, M.S. Aboodi, G.L. Kaluza, et al., Vascular response to zotarolimus-coated balloons in injured superficial femoral arteries of the familial hypercholesterolemic swine, *Circ-Cardiovasc. Interv.* 4 (5) (2011) 447–455.
- [9] P.P. Buszman, K. Milewski, A. Zurakowski, J. Pajak, M. Jelonek, P. Gasior, A. Peppas, et al., Experimental evaluation of pharmacokinetic profile and biological effect of a novel paclitaxel microcrystalline balloon coating in the iliofemoral territory of swine, *Catheter. Cardiovasc. Interv.* 83 (2) (2014) 325–333.
- [10] P.P. Buszman, A. Tellez, M. Afari, Y.P. Cheng, G.B. Conditt, J.C. McGregor, K. Milewski, et al., Stent healing response following delivery of paclitaxel via durable polymeric matrix versus iopromide-based balloon coating in the familial hypercholesterolaemic swine model of coronary injury, *EuroIntervention* 9 (4) (2013) 510–516.
- [11] R. Waksman, R. Pakala, Drug-eluting balloon: the comeback kid?, *Circ Cardiovasc. Interv.* 2 (4) (2009) 352–358.
- [12] A. De Labriolle, R. Pakala, L. Bonello, G. Lemesle, M. Scheinowitz, R. Waksman, Paclitaxel-eluting balloon: from bench to bed, *Catheter. Cardiovasc. Interv.* 73 (5) (2009) 643–652.
- [13] T. Heilmann, C. Richter, H. Noack, S. Post, D. Mahnkopf, A. Mittag, H. Thiele, et al., Drug release profiles of different drug-coated balloon platforms, *Eur. Cardiol. Rev.* 6 (4) (2010) 40–44.
- [14] J.P. Sur, I.P. Casserly, H.S. Gurm, Balloon and stent technology, in: I.P. Casserly, R. Sachar, J.S. Yadav (Eds.), *Practical Peripheral Vascular Intervention*, second ed., LWW, Philadelphia, 2011.
- [15] S. Lancaster, S. Kakade, G. Mani, Microrough cobalt-chromium alloy surfaces for paclitaxel delivery: preparation, characterization, and in vitro drug release studies, *Langmuir* 28 (31) (2012) 11511–11526.
- [16] S. Lamichhane, A. Gallo, G. Mani, A polymer-free paclitaxel eluting coronary stent: effects of solvents, drug concentrations and coating methods, *Ann. Biomed. Eng.* 42 (6) (2014) 1170–1184.
- [17] G. Mani, C.E. Macias, M.D. Feldman, D. Marton, S. Oh, C.M. Agrawal, Delivery of paclitaxel from cobalt-chromium alloy surfaces without polymeric carriers, *Biomaterials [Article]* 31 (20) (2010) 5372–5384.
- [18] A. Gallo, G. Mani, A stent for co-delivering paclitaxel and nitric oxide from abluminal and luminal surfaces: preparation, surface characterization, and in vitro drug release studies, *Appl. Surf. Sci.* 279 (2013) 216–232.
- [19] S. Kakade, G. Mani, A comparative study of the effects of vitamin C, sirolimus, and paclitaxel on the growth of endothelial and smooth muscle cells for cardiovascular medical device applications, *Drug Des. Devel. Ther.* 7 (2013) 529–544.
- [20] S. Lamichhane, S. Lancaster, E. Thirupathi, G. Mani, Interaction of endothelial and smooth muscle cells with cobalt-chromium alloy surfaces coated with paclitaxel deposited self-assembled monolayers, *Langmuir* 29 (46) (2013) 14254–14264.
- [21] S. Kern, H.Z. Feng, H.G. Wei, S. Cala, J.P. Jin, Up-regulation of alpha-smooth muscle actin in cardiomyocytes from non-hypertrophic and non-failing

- transgenic mouse hearts expressing N-terminal truncated cardiac troponin I, *FEBS Open Biol.* 4 (2014) 11–17.
- [22] M. Gupta, A. Korol, J.A. West-Mays, Nuclear translocation of myocardin-related transcription factor-A during transforming growth factor beta-induced epithelial to mesenchymal transition of lens epithelial cells, *Mol. Vision* 19 (2013) 1017–1028.
- [23] L.M. Fernandes, F.B. Teixeira, S.M. Alves-Junior, J.J. Pinheiro, C.S. Maia, R.R. Lima, Immunohistochemical changes and atrophy after chronic ethanol intoxication in rat salivary glands, *Histol. Histopathol.* 30 (9) (2015) 1069–1078.
- [24] R.A. Byrne, M. Joner, F. Alfonso, A. Kastrati, Drug-coated balloon therapy in coronary and peripheral artery disease, *Nat. Rev. Cardiol.* 11 (1) (2014) 13–23.
- [25] M.C. Berg, H. Kolodziej, B. Cremers, G. Gershony, U. Speck, Drug-coated angioplasty balloon catheters: coating compositions and methods, *Adv. Eng. Mater.* 14 (3) (2012) B45–B50.
- [26] N. Gondaliya, D.K. Kanchan, P. Sharma, P. Joge, Structural and conductivity studies of poly(ethylene oxide)–silver triflate polymer electrolyte system, *Mater. Sci. Appl.* 2 (2011) 1639–1643.
- [27] M. Khenfouch, M. Baitoul, H. Aarab, M. Maaza, Morphological, vibrational and thermal properties of confined graphene nanosheets in an individual polymeric nanochannel by electrospinning, *Graphene* 1 (2) (2012) 15–20.
- [28] S.E. Stoebner, G. Mani, Effect of processing methods on drug release profiles of anti-restenotic self-assembled monolayers, *Appl. Surf. Sci.* 258 (12) (2012) 5061–5072.
- [29] G. Mani, N. Torres, S. Oh, Paclitaxel delivery from cobalt-chromium alloy surfaces using self-assembled monolayers, *Biointerphases* 6 (2) (2011) 33–42.
- [30] E. Thiruppathi, G. Mani, Vitamin-C delivery from CoCr alloy surfaces using polymer-free and polymer-based platforms for cardiovascular stent applications, *Langmuir* 30 (21) (2014) 6237–6249.
- [31] F.S. Fay, K. Fujiwara, D.D. Rees, K.E. Fogarty, Distribution of alpha-actinin in single isolated smooth muscle cells, *J. Cell Biol.* 96 (3) (1983) 783–795.
- [32] D.S. Zhang, L. Sun, W. Xian, F.Y. Liu, G.H. Ling, L. Xiao, Y.H. Liu, et al., Low-dose paclitaxel ameliorates renal fibrosis in rat UUO model by inhibition of TGF-beta/Smad activity, *Lab Invest. [Article]* 90 (3) (2010) 436–447.
- [33] L. Zhang, X. Xu, R. Yang, J. Chen, S. Wang, J. Yang, X. Xiang, et al., Paclitaxel attenuates renal interstitial fibroblast activation and interstitial fibrosis by inhibiting STAT3 signaling, *Drug Des. Devel. Ther.* 9 (2015) 2139–2148.
- [34] L.E. van Vlerken, T.K. Vyas, M.M. Amiji, Poly(ethylene glycol)-modified nanocarriers for tumor-targeted and intracellular delivery, *Pharm. Res.* 24 (8) (2007 Aug) 1405–1414.
- [35] T. Yamaoka, Y. Tabata, Y. Ikada, Distribution and tissue uptake of poly(ethylene glycol) with different molecular weights after intravenous administration to mice, *J. Pharm. Sci.* 83 (4) (1994) 601–606.
- [36] L.L. Ma, L. Deng, J.M. Chen, Applications of poly(ethylene oxide) in controlled release tablet systems: a review, *Drug Dev. Ind. Pharm.* 40 (7) (2014) 845–851.
- [37] B.D. Ratner, A.S. Hoffman, F.J. Schoen, J.E. Lemons, *Biomaterials Science: An Introduction to Materials in Medicine*, second ed., Elsevier Academic Press, London, 2004.